DISCLAIMER

This report was prepared as an account of work sponsored by an agency of the United States Government. Neither the United States Government nor any agency thereof, nor any of their employees, makes any warranty, express or implied, or assumes any legal liability or responsibility for the accuracy, completeness, or usefulness of any information, apparatus, product, or process disclosed, or represents that its use would not infringe privately owned rights. Reference herein to any specific commercial product, process, or service by trade name, trademark, manufacturer, or otherwise does not necessarily constitute or imply its endorsement, recommendation, or favoring by the United States Government or any agency thereof. The views and opinions of authors expressed herein do not necessarily state or reflect those of the United States Government or any agency thereof. Reference herein to any social initiative (including but not limited to Diversity, Equity, and Inclusion (DEI); Community Benefits Plans (CBP); Justice 40; etc.) is made by the Author independent of any current requirement by the United States Government and does not constitute or imply endorsement, recommendation, or support by the United States Government or any agency thereof.

A U.S. DEPARTMENT OF ENERGY NATIONAL LAB • SAVANNAH RIVER SITE • AIKEN, SC • USA

Hydrochlorination of Uranium Dioxide in a Molten Salt Mixture- Phase 2: Sparged Benchtop Reaction Vessel Experiments

V. T. Nguyen

N. Hege

B. J. Foley

R. A. Pierce

April 2025

SRNL-STI-2025-00192, Revision 0

DISCLAIMER

Printed in the United States of America

Prepared for
U.S. Department of Energy

SRNL-STI-2025-00192
Revision 0

Keywords: *Uranium Dioxide, Molten Salt, Uranium Chlorination, Hydrochlorination, GAIN*

Retention: *Varies*

Hydrochlorination of Uranium Dioxide in a Molten Salt Mixture- Phase 2: Sparged Benchtop Reaction Vessel Experiments

V. T. Nguyen
N. Hege
B. J. Foley
R. A. Pierce

April 2025

Savannah River National Laboratory is operated by Battelle Savannah River Alliance for the U.S. Department of Energy under Contract No. 89303321CEM000080.

REVIEWS AND APPROVALS

AUTHORS:

_____
V. T. Nguyen, SRNL-ELM-SS&E Date

_____
N. Hege, SRNL-ELM-SS&E Date

_____
B. J. Foley, SRNL-GSD-ET&A Date

_____
R. A. Pierce, SRNL-ELM-SS&E Date

TECHNICAL REVIEW:

_____
T. C. Shehee, SRNL-ELM-SS&E Date

APPROVAL:

_____
G. A. Morgan, Manager Date
SRNL-ELM-SS&E

_____
F. Pennebaker, Director Date
SRNL-ELM

PREFACE OR ACKNOWLEDGEMENTS

We would like to thank Citiyah Burton, Alaina Bodie, and Rebecca Carter for their assistance during the following experiments. We are grateful for the funding provided by the DOE GAIN program. And lastly, we are thankful to the Metatomic® Inc. team (Ken Baer, Steve Hung, Mike Stake, Tom Epting, Tor Osmundsen) for the opportunity to support the development of nuclear energy technology.

EXECUTIVE SUMMARY

In 2023, Metatomic® Inc., a South Carolina based company, was awarded a Gateway for Advanced Innovation in Nuclear (GAIN) research voucher for a proposed series of experiments aimed at demonstrating the viability of a spent nuclear fuel (SNF) recycling process patented by Metatomic® Inc. For the GAIN voucher, Metatomic® Inc. selected Savannah River National Laboratory (SRNL) as a partner in executing the proposed proof-of-concept experiments. This report outlines the proof-of-concept experiments performed by SRNL for Metatomic® Inc. during Phase 2 (of 2) experimentation.

Though Phase 1 provided evidence of successful hydrochlorination, Phase 2 highlighted the nuances and challenges associated with scaling the reaction. The target UCl_4 species generated by the hydrochlorination of UO_2 generates water, which consumes UCl_4. Compared to the single datapoint obtained at the end of the Phase 1 experiments, data collected at multiple timepoints during Phase 2 experiments indicated a presumed maximum percent conversion of 23% for this system that is likely influenced by water generation. Engineering improvements might be able to increase the percent conversion, but not likely to the degree needed for successful implementation of the technology. Moisture also presents an issue for the Hastelloy C276 reaction vessel. Eventually, corrosion will compromise the integrity of the reaction vessel, and the corrosion products could potentially affect the hydrochlorination chemistry. The presence of corrosion products, which were not produced in the Phase 1 alumina crucible, can and have created challenges when analyzing samples.

Hydrochlorination of UO_2 using anhydrous HCl appears to be hindered by its own success through the generation of water. If continued focus on the target reaction is desired, managing water must be a priority to increase percent conversion and reduce corrosion of the Hastelloy C276 vessel. Regardless, aside from a perfect exclusion of water, the effects of moisture on the current system will eventually compound. Given the current challenges relate to the chemistry of the reaction, an engineering solution would not likely not solve this system's current issues. An alternative reaction that does not generate water would be recommended. Carbon tetrachloride and phosgene are two chemicals which have been shown to be effective at converting UO_2 to UCl_4 without the generation of water.

TABLE OF CONTENTS

LIST OF TABLES

LIST OF FIGURES

LIST OF ABBREVIATIONS

CAD	Computer-Aided Design
DOE	Department of Energy
GAIN	Gateway for Accelerated Innovation in Nuclear
HCl	Hydrogen Chloride
IBI	International Bio-analytical Industries Inc.
IC-Anions	Ion Chromatography Anions
ICP-MS	Inductively Coupled Plasma Mass Spectrometry
LOD	Limit of Detection
NAA	Neutron Activation Analysis
pXRD	Powder X-Ray Diffraction
RPM	Rotations per Minute
SRNL	Savannah River National Laboratory
UV-vis	Ultraviolet-Visible light

1.0 Introduction

To support innovation in nuclear technology, the Department of Energy (DOE) awarded Metatomic® Inc. with a Gateway for Accelerated Innovation in Nuclear (GAIN) voucher in 2023 to support commercialization of their patent.[1] A collaboration with the Savannah River National Lab (SRNL) was made to characterize the molten salt immersed UO_2 hydrochlorination subsystem. Proof-of-concept research on the hydrochlorination of UO_2 by reaction with anhydrous hydrogen chloride (HCl) gas in a molten salt medium was performed on a laboratory bench scale.[1,2] Per the commercial goals of Metatomic® Inc., experimental conditions and designs were selected to minimize the production of oxygen-containing side products. A eutectic salt mixture of NaCl-CsCl was selected to promote the formation of oxygen-free uranium chloride species. The intended chemical reaction is listed in Equation 1:

$$UO_2(s) + 4HCl(g) \xrightarrow{\Delta} UCl_4(sln) + 2H_2O(g) \qquad \text{Equation 1}$$

Project milestones were divided into two phases. Phase 1 involved a preliminary small-scale assessment of the hydrochlorination process using a tube furnace. The primary goal of Phase 1 was to assess the feasibility of the hydrochlorination reaction, probe the effect of furnace temperature, and evaluate the applicability of available analytical techniques. The Phase 1 hydrochlorination experiments consisted of weighing UO2 into alumina crucibles with a eutectic mixture of NaCl and CsCl, heating the uranium/salt mixture to a varied temperature (550, 650, or 750 °C), and flowing HCl gas across the surface of the uranium-bearing molten salt mixture. Results from the Phase 1 experiments indicated that hydrochlorination of UO_2 to UO_2Cl_2 and UCl_4 in molten salt media was achieved. Based on a 23.1% conversion to water-soluble U species that was expected to favor the U(IV) species[3] while minimizing salt volatility, a 650 °C hydrochlorination temperature was selected for Phase 2. Results from the Phase 1 experiments have been previously documented.[4]

This report details the results from the Phase 2 experiments, which involved a scaled-up hydrochlorination apparatus in a custom-built, bench-scale reactor. Conditions, such as HCl flow rate, starting UO_2 content, additional compounds, and HCl sparging strategies were assessed at several timepoints during hydrochlorination. The additional compounds that were added were selected to represent some of the fission products expected in used nuclear fuel.[5,6] Promising analytical techniques from Phase 1 were utilized to gauge the degree of hydrochlorination.[4]

2.0 Experimental Procedure

2.1 General Experimental Apparatus

For the following Phase 2 experiments, the experimental apparatus was assembled as described below. Deviations to this setup are specified in the corresponding experimental section. The reaction liner, vessel lid, vessel body, furnace, and stir motor assembly were procured by Metatomic and produced by Col-Int Tech/Vivtek Instruments. The vessel liner and vessel lid were made of a Hastelloy C276 alloy. The vessel body was fabricated from 304L stainless steel. All other items were procured by or manufactured by SRNL.

A Hastelloy C276 reaction vessel liner (L=170 mm, 500 mL capacity) was utilized for the molten salt hydrochlorinations (Figure 1A). As depicted in Figure 1B and C, the reaction vessel liner was inserted into a flanged stainless vessel body (L=180 mm, 5 mm thickness). The flanged vessel body can be secured to the Hastelloy C276 vessel lid (Figure 2) using six screws (S1). Three jack screws (S2) on the vessel lid were designed to assist in the separation of the vessel lid and the vessel body. The threads of both the S1 and S2 screws were lightly coated in a high temperature silicone-based lubricant. Either a Hastelloy C276

gasket and/or aluminum oxide fiber gaskets were used between the reaction vessel liner and the reaction lid to create a seal.

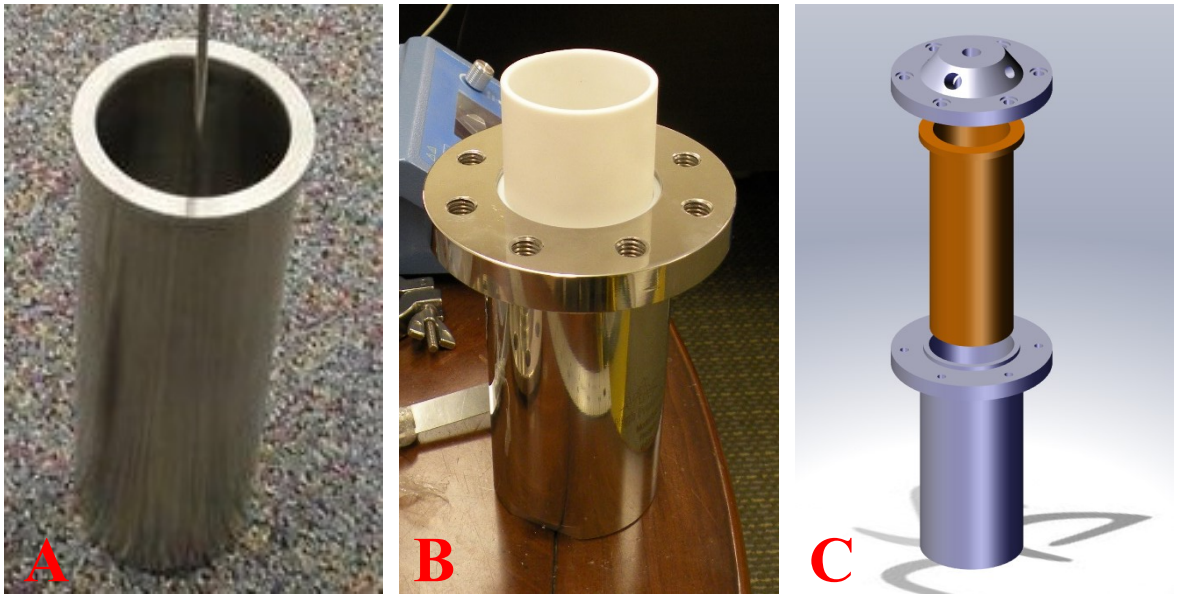

Figure 1. A) Hastelloy C276 reaction vessel liner. B) 316L-Stainless steel vessel body. C) Graphic of vessel liner inserted into vessel body and capped with the vessel lid.

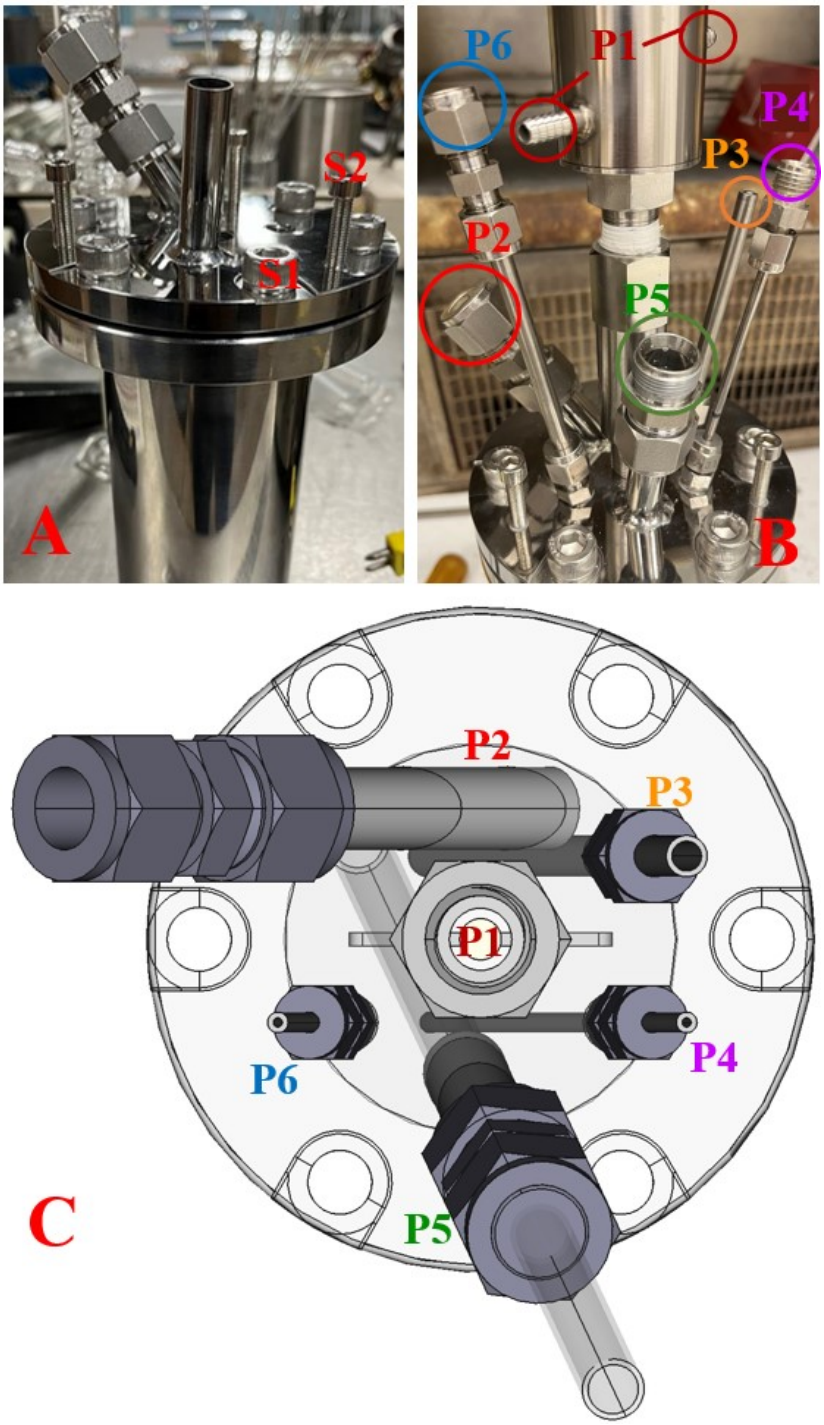

Figure 2. A) Vessel lid secured to flanged vessel body with six screws (S1) and equipped with three jack screws (S2). B) Vessel lid with stir motor assembly and ports for cooling (P1), off-gas exhaust (P2), thermowell (P3), sparge tube (P4), sampling port (P5), and cover gas port (P6). C) Computer-Aided Design (CAD) of vessel lid.

The vessel lid has six ports (P1-P6) to manage the hydrochlorination experiment. The central port (P1) was designed to fit the magnetic stir motor assembly. The stir motor assembled was setup to be air-cooled for the hydrochlorination experiments. Reaction off-gases were passed through a ½ in. Hastelloy C276 tube

with a Swagelok union adapter (P2). P3 was designed as a thermowell to house a Type K thermocouple. For the thermowell, a ¼ in. Hastelloy C276 tube, with one end closed, was inserted through the vessel lid using a pass-through Swagelok connector. A ⅛ in. Hastelloy C276 rod was also inserted through P4 using a pass-through Swagelok connector which functioned as a sparge tube. This tube allowed anhydrous HCl or argon gas flow to be sparged towards the bottom of the reaction vessel liner. A short length of a ½ in. Hastelloy C276 tube was welded to the vessel lid (P5). A ½ in. Swagelok union allowed for a ¼ in. threaded Hastelloy C276 rod to be inserted through the vessel lid. This provided for sampling of the molten salt throughout the experiment. During the hydrochlorination process, P5 could be closed using a cap nut. The final port, P6, fed a cover gas (argon) to be delivered directly above the molten salt mixture.

Since P4 and P6 had flexible Teflon tubing for plumbing gases, these two ports had several inches of Hastelloy C276 tubing extending above the reaction lid. This ensured radiating heat protection from the vessel so it would not compromise the integrity of the Teflon tubes. In addition, argon gas flow through the Teflon tubing provided cooling. For ports P2, P3, and P4, graphite ferrules were used on the Swagelok components. Following hydrochlorination experiments, disassembly of the vessel was performed after the vessel cooled to room temperature. Since the Hastelloy C276 rods inserted through P2 and P3 would have been challenging to remove from a solidified salt matrix, graphite ferrule usage would allow for the separation of the vessel lid from the rest of the reaction apparatus. For P4, graphite ferrules allowed for a seal to form with a quartz tube for off-gas exhaust management. All ports were designed at an angle to accommodate the stir motor assembly (Figure 3) and to simplify operations for the researchers.

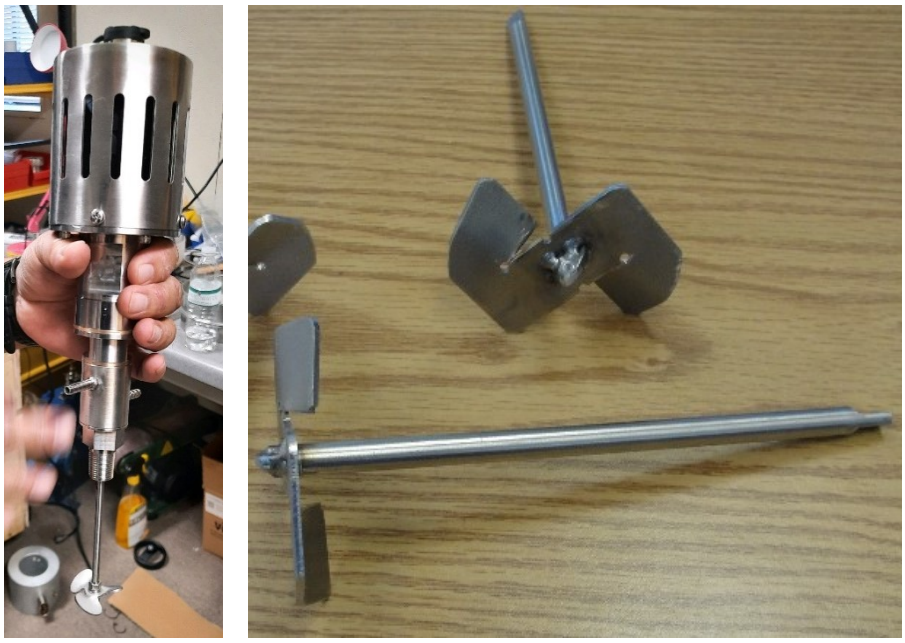

Figure 3. Left) Magnetic stir motor assembly. Right) Stir impellor with a beveled shaft.

Depicted in Figure 3 is the magnetic stir motor assembly attached at P1. Hastelloy C276 impellors and beveled shafts were employed. A Swagelok union with a graphite ferrule was used to secure the stir shaft and impellor to the magnetic motor assembly. The use of graphite ferrules was for similar reasons as previously mentioned for P2 and P3. To align the stir shaft with the magnetic stir motor, the stir shaft was beveled to key into a slot on the stir motor assembly. An internal view of the reaction vessel liner was depicted in Figure 4 to illustrate that all inserted tubes would not interfere with the stirring mechanism, when situated above the stir impellor.

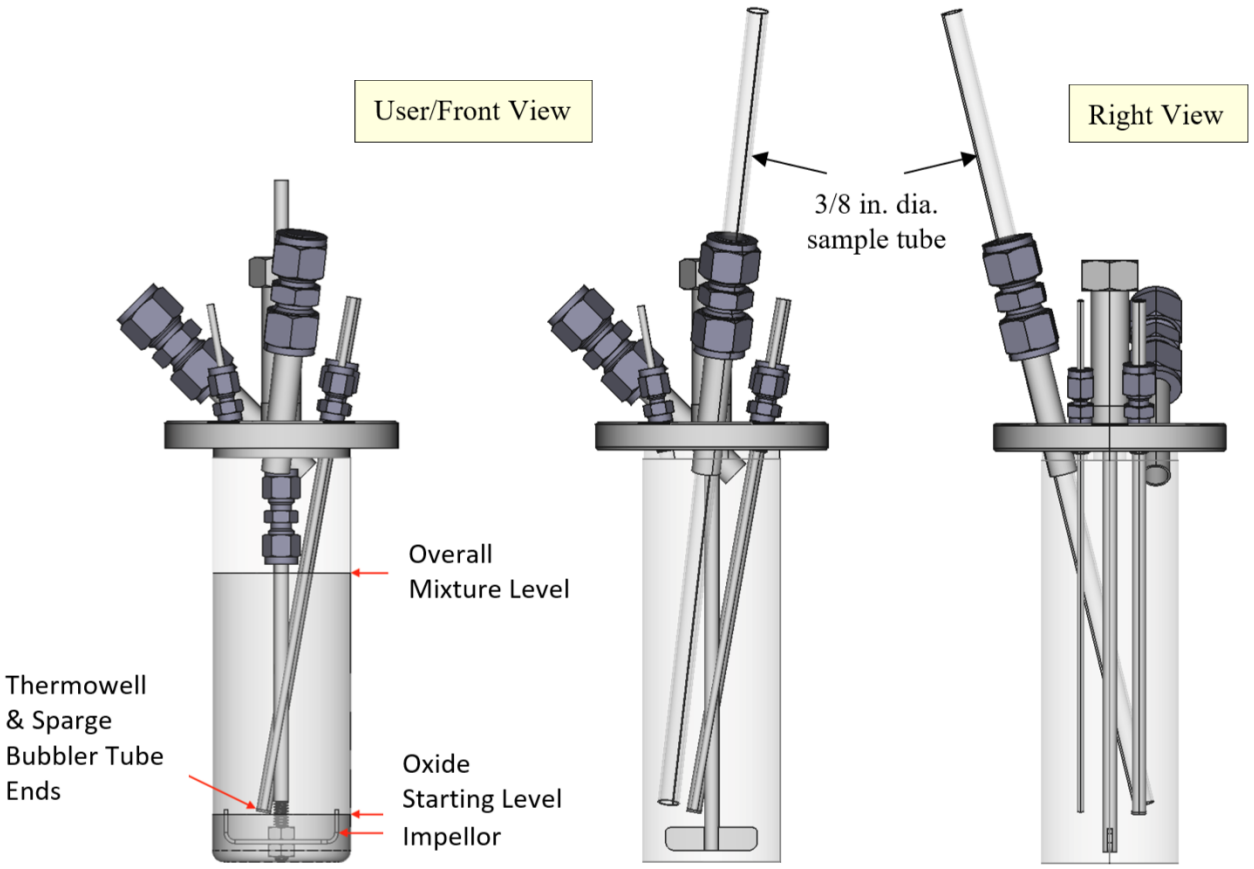

Figure 4. Front and right-side view of the vessel liner and vessel lid.

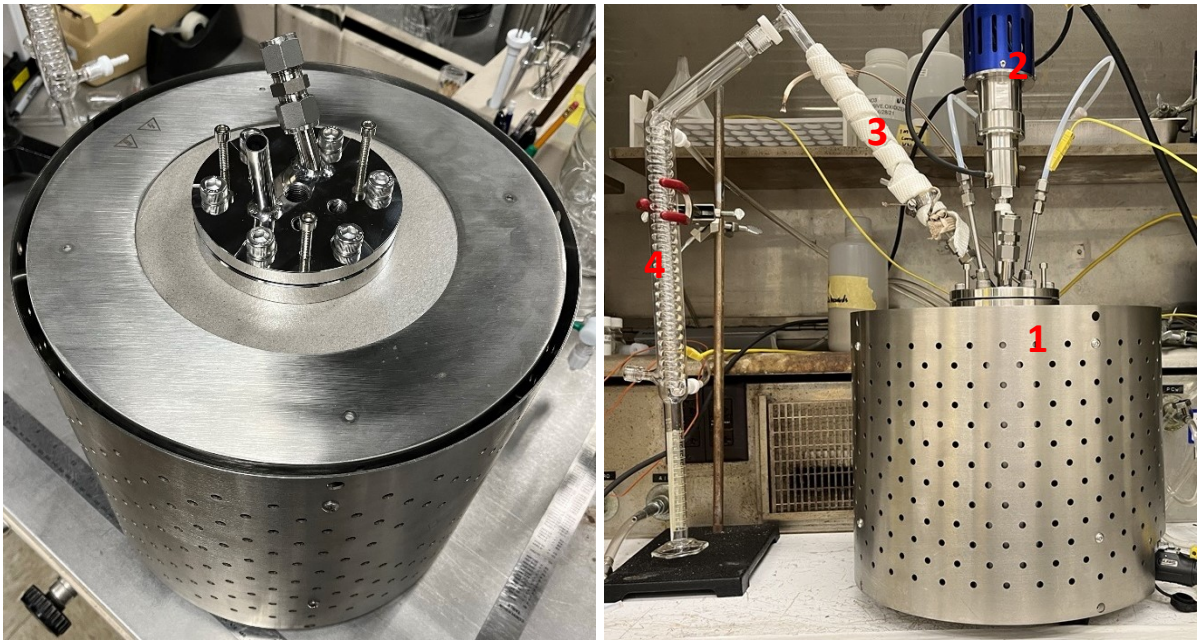

Figure 5. Vessel body with vessel lid placed into a stainless-steel heating furnace (1) equipped with a stir motor assembly (2), quartz salt condenser (3), and water condenser (4).

The vessel lid and vessel body were then inserted into a stainless-steel heating furnace (Figure 5) that was insulated with alumina fibers. A quartz tube wrapped in heating tape was secured to P2 using a Swagelok nut with a graphite ferrule. The quartz tube was designed with two thermocouples near the inlet and the outlet (Figure 6). This tube, or salt condenser, was designed to collect volatilized solids from the vessel liner.

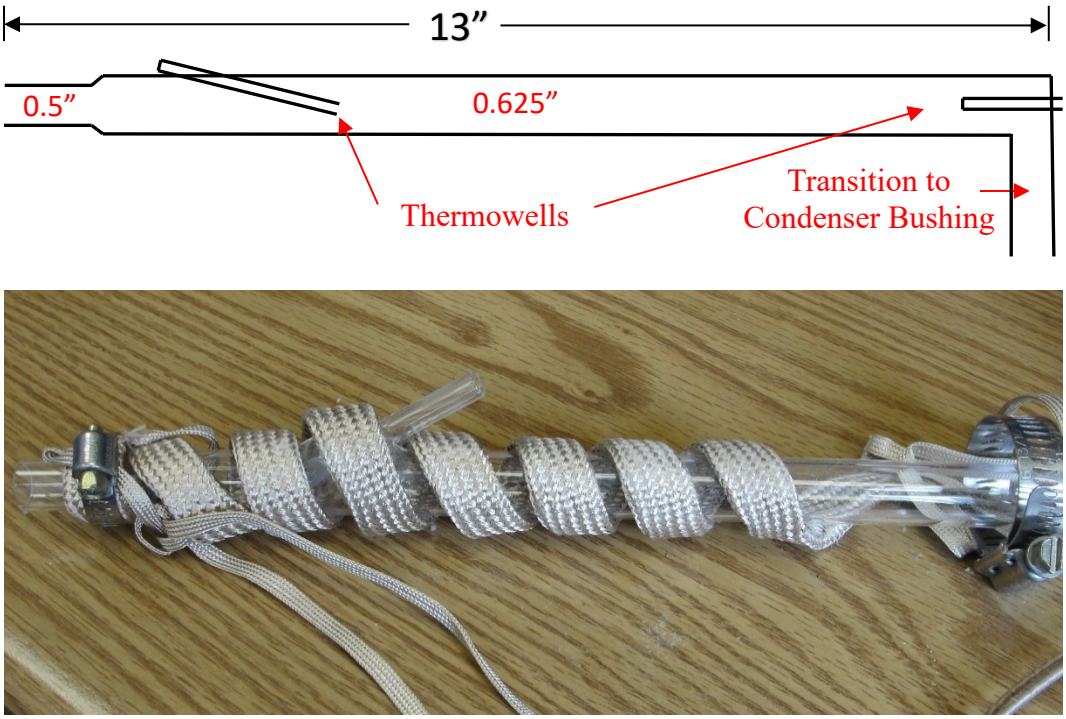

Figure 6. Top) Schematic of salt condenser. Bottom) Schematic of quartz tube wrapped in heating tape.

Downstream of the salt condenser was a water condenser (Figure 7) designed to collect the expected water byproduct generated from the UO_2 hydrochlorination reaction. This measurement was utilized as an observable metric to monitor the progression of the reaction in real-time. Coils within the water condenser allowed for process water to be used for cooling. The water condenser was modified to include a graduated cylinder to collect and measure accumulated condensation. The exhaust from the water condenser was then passed through a collection vessel and two scrubber bottles to capture hazardous off-gas products (Figure 8). The collection bottle acted as a precautionary repository for any solutions from the scrubber bottles that may backflow during sampling. The two scrubber bottles were designed to neutralize unreacted HCl gas. Both bottles were attached in series and were filled with 5 M sodium hydroxide (NaOH) solutions. Coarse frits within the scrubber bottles allowed incoming gases to sparge through the caustic solution as bubbles. The experimental apparatus was located in a fume hood designed to handle radiological materials safely.

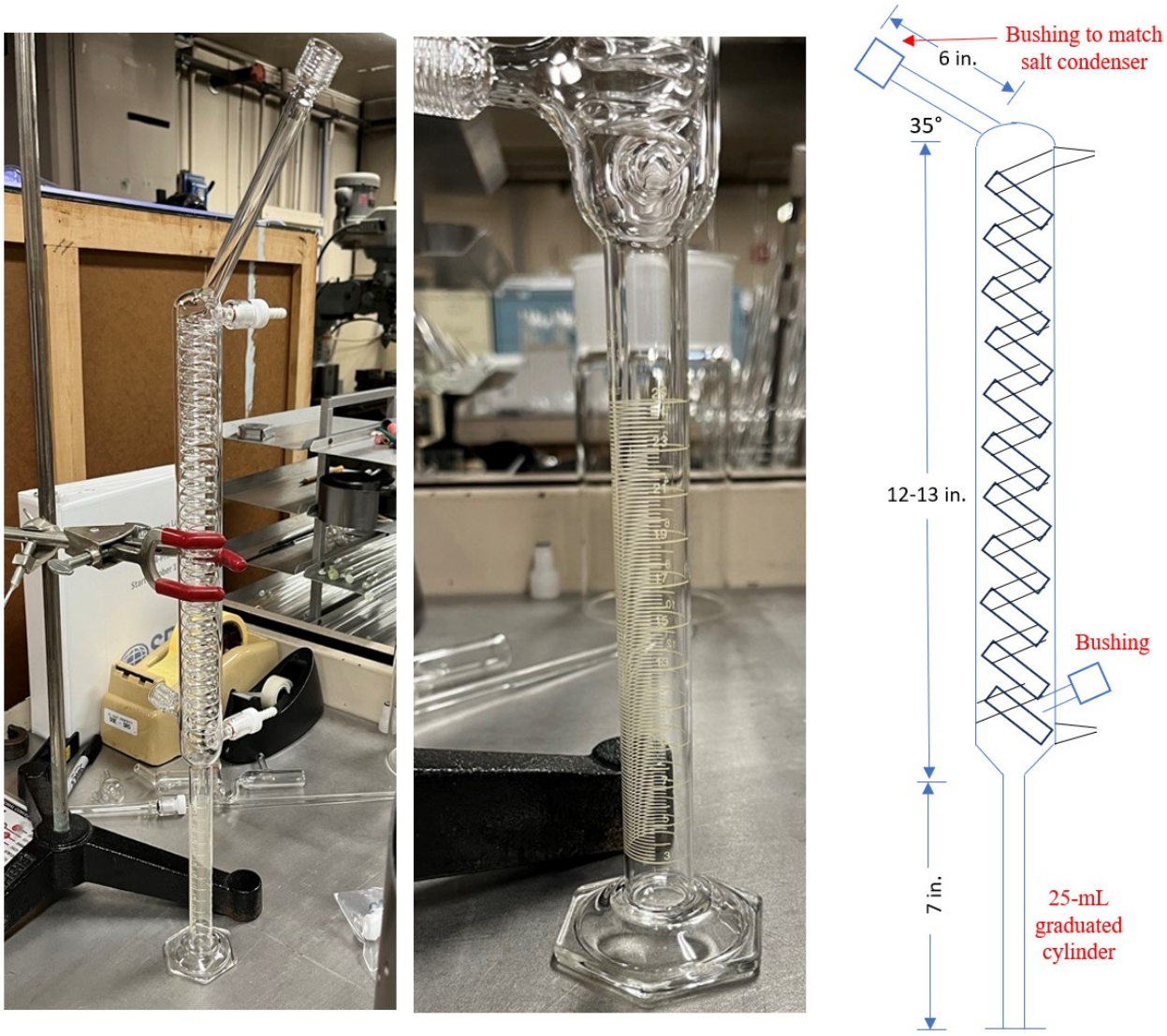

Figure 7. Water-cooled capture condenser that has been modified to measure collected condensates.

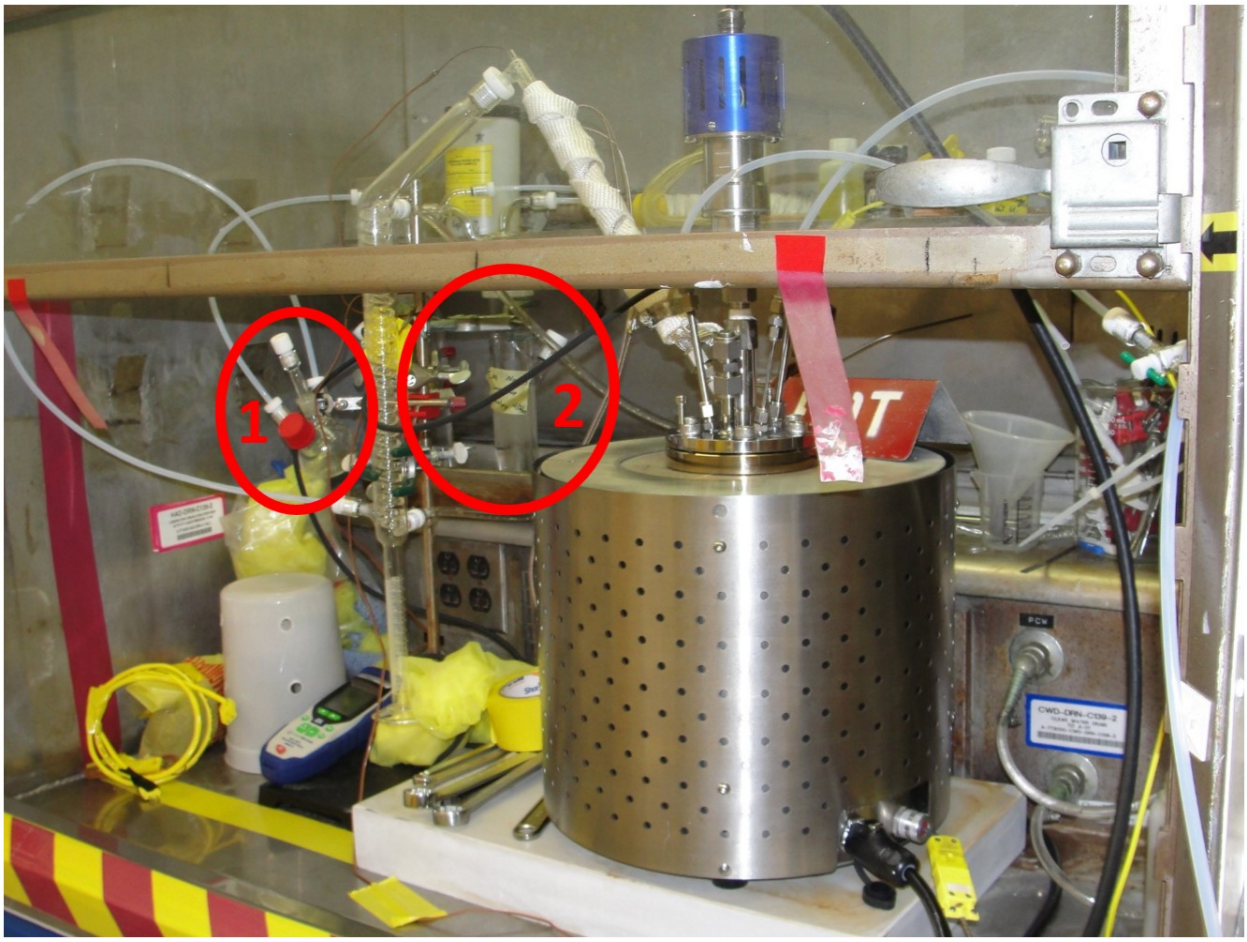

Figure 8. Experimental apparatus setup within a fume hood designed to handle radiological materials and to handle HCl gas with a round bottom flask collection vessel (1) and two scrubber bottles in series (2).

Argon and HCl gas control was managed in a non-radiological fume hood (Figure 9A). An HCl gas cylinder was utilized to periodically inflate a Tedlar bag. Flow of HCl gas to the vessel liner was metered with a calibrated peristaltic pump. Argon gas flow was controlled and measured with a PTFE-based flowmeter. Gas management through either the sparge tube (P3) or cover gas inlet (P6) could be further controlled by a system of Ts with stopcocks (Figure 9B).

System temperature and the stir motor were managed by thermocouples, temperature controllers, and a tachometer (Figure 9C) located inside a radiological buffer area. The reaction furnace heating was moderated by a temperature controller. The temperature in the vessel liner was measured by a thermocouple which was inserted into the thermowell (P3). A tachometer was used to set and measure the rotations per minute (RPM) of the stirring. The salt condenser temperature was regulated by heating tape and a temperature controller. The temperatures at the inlet and outlet thermowells of the salt condenser were measured by Type K thermocouples located inside the radiological hood. A simplified diagram of the overall experimental apparatus can be visualized in Figure 10.

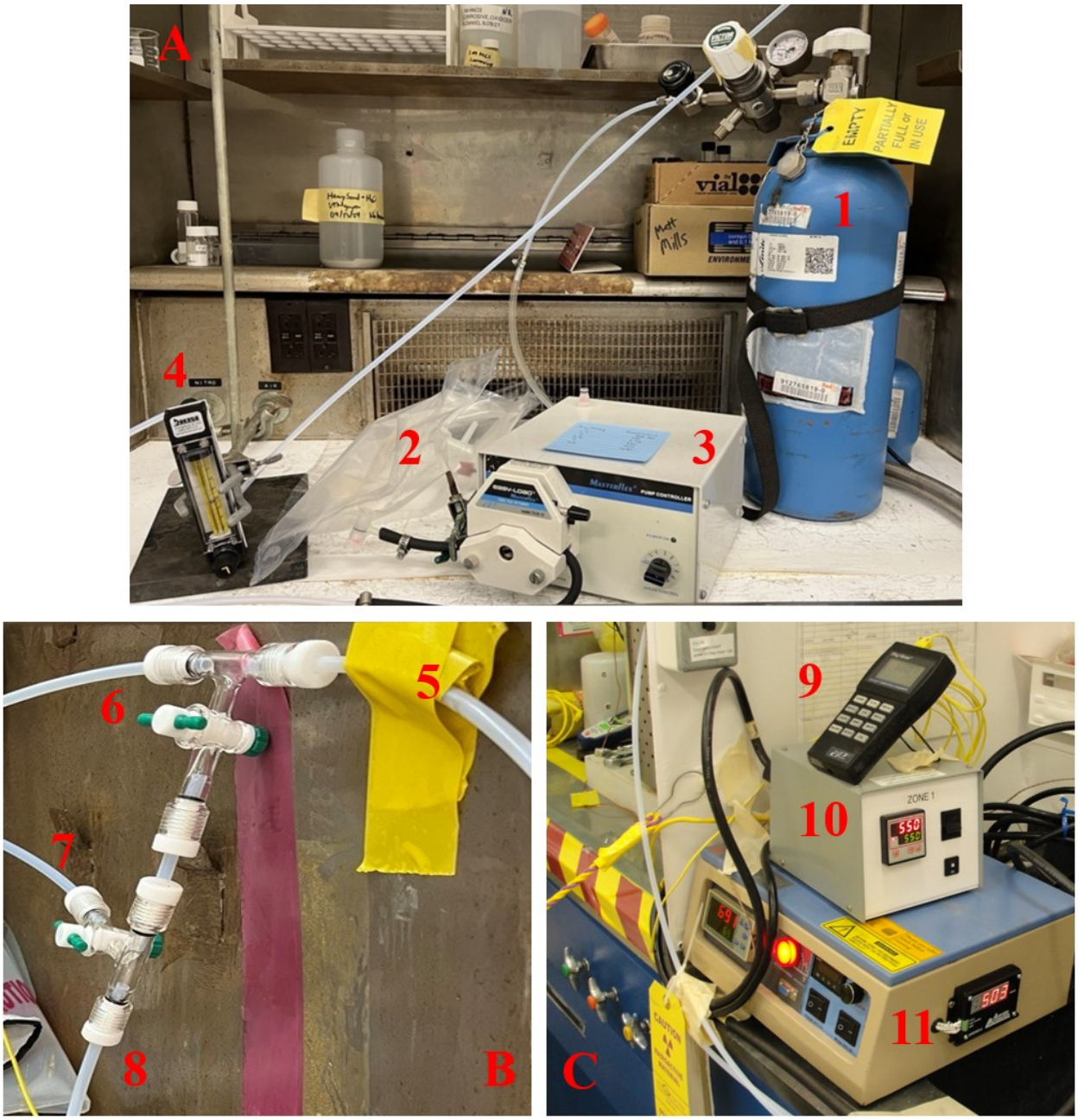

Figure 9. A) Gas management setup within a fume hood, including an HCl gas cylinder (1), Tedlar bag (2), peristaltic pump for HCl gas (3), and flowmeter for argon gas (4). B) T-valve with stopcocks to manage HCl (5) and argon gas (6) flow through either the sparge tube (7) and/or cover gas inlet (8). C) Thermocouple (9), temperature controller for the salt condenser (10), and temperature/stir assembly controller for the reaction vessel (11).

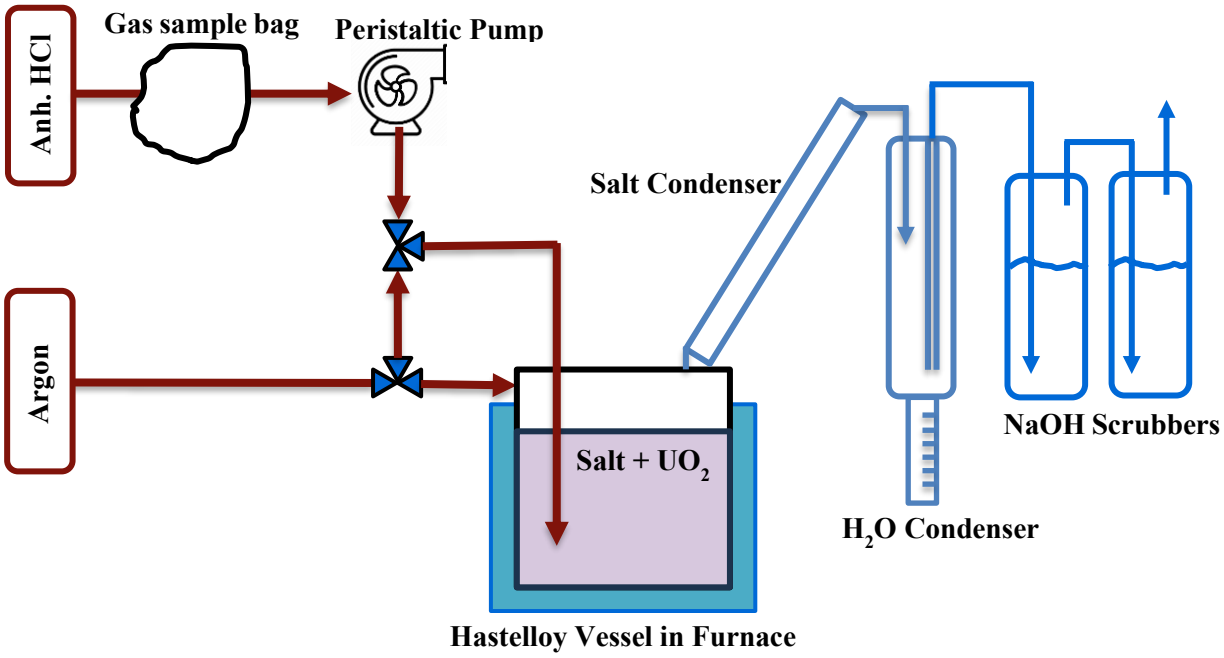

Figure 10. Schematic of the overall experimental apparatus.

2.2 General Experimental Conditions

Uranium dioxide (UO_2) was purchased from International Bio-analytical Industries Inc. All experiments involved a salt matrix composed of sodium chloride (NaCl) and cesium chloride (CsCl). Necessary masses of NaCl, CsCl, UO_2, or fission product simulants for each experiment were weighed on analytical balances. To prepare the reaction vessel, the furnace was set to ramp the temperature at a rate of 20 °C/min. The temperature of the reaction vessel during hydrochlorination was 670 ± 25°C. The argon gas flow throughout the system was kept at 50 mL/min during all heating, hydrochlorination, and cooling steps. The salt condenser was heated to 550 °C.

The procedure for obtaining a molten salt sample from the reaction vessel liner involved pausing the HCl gas flow by turning off the peristaltic pump. Sequentially, the cap nut was removed from P5 with a deep-set nut driver, and a ¼ in. threaded Hastelloy C276 rod was inserted into the reaction vessel liner. The sample dip rod was then removed, the cap nut was replaced, and the HCl gas flow was resumed. The solidified salt matrix on the sample dip rod was then dissolved in a pre-weighed (~20 g) amount of water inside a centrifuge tube. Then, the centrifuge tube with the dissolved molten salt sample was weighed on an analytical balance. Approximately 8 mL of the solution in the centrifuge tube was filtered through a 0.45-micron PTFE syringe filter. A 4.5 mL aliquot of this filtered solution was mixed with 0.5 mL of a 10 M nitric acid (HNO_3) solution to create a 1 M HNO_3 solution. This solution was analyzed via UV-vis spectroscopy. If necessary, dilutions of this solution were prepared and spectra at multiple timepoints were collected. If a sample was to be submitted for ICP-MS analysis, a small aliquot (<2 mL) of the 1 M HNO_3 solution was submitted.

The procedure for obtaining a sample from the scrubber solutions involved opening a side port on the scrubber bottle. A plastic syringe was utilized to obtain several milliliters of sample. To obtain samples for powder X-ray Diffraction (pXRD) analysis, the sample dip rod was dipped three times through the sampling

port to get a representative sample. The resulting salt matrix that solidified onto the threaded rod was scraped off and submitted for analysis.

Once the hydrochlorination experiment was complete, the peristaltic pump for HCl gas flow and temperature controllers were turned off. Argon gas flowed through the cover gas inlet while the system cooled down overnight. Samples of the water condensate in the graduated cylinder were collected at the end of each experiment. The contents of the graduated cylinder were decanted through the outlet of the water condenser.

2.3 Experiment 1: Uranium Salt Bridge

Details for Experiment 1 are listed below. The experimental method was performed according to Section 2.2 with the following exceptions mentioned.

The experimental apparatus was secured as described using a single Hastelloy C276 gasket to create a seal between the vessel lid and vessel liner. A eutectic salt mixture of NaCl and CsCl was prepared with the masses listed in Table A 1. The two salts were well-mixed and added to the vessel liner. The mass of UO_2 in Table A 1 was then added to the vessel liner on top of the salt matrix. For the scrubber bottles, scrubber bottle 1 was placed first in series and was filled to a maximum of 300 mL of 5 M NaOH solution. Scrubber bottle 2 was filled to a maximum of 167 mL of 5 M NaOH solution. Bubbles emerging through the frit of the scrubber bottles indicated argon gas flow through the system.

Once the contents of the vessel liner temperature stabilized at 650 °C, the HCl gas flow rate and stir rate were set according to Table 1. Samples were collected every thirty minutes by inserting the sample dip rod through the sampling port. A layer of resistance was noted when inserting the sample dip rod for the first sample. Upon removal from the vessel liner, the sample on the sample dip rod appeared completely solid, rather than liquid. The collected solids were bright blue in color (Figure 11). These solids were added to pre-weighed centrifuge tubes with water (Table A 2), and then the mixtures were reweighed again to collect the mass of the dip sample. Once mixed with water, the samples appeared as clear solutions with some insoluble black/brown precipitates. The samples were filtered, acidified, and analyzed via UV-vis spectroscopy per the general experimental conditions discussed. A pXRD sample was collected at the 4-h timepoint and immediately analyzed. Though a target stir rate of either ~250 rpm or ~500 rpm was targeted, there was no evidence that the impellor was stirring. Inserting the sample dip rod to the bottom of the vessel liner, and in the pathway of the impellor, resulted in no perceivable interruption of the stirring. Furthermore, the digital readout of the tachometer did not reduce to 0 rpm when inserting the sample dip rod to the bottom the vessel liner. This suggests the tachometer output was not representative of the impellor stirring.

Table 1. Timepoints and the corresponding HCl gas flow rate.

Condition	Timeframe (h)	HCl flow rate (mL/min)
1	0-1	50
2	1-2	50
3	2-3	125
4	3-4	125
5	4-5	200
6	5-6	200

Figure 11. Sample collected on Hastelloy rod being mixed in water.

After the reaction vessel was cooled to room temperature, disassembly of the experimental apparatus revealed the salt condenser had minimal amounts of salt (Figure 12A). The six screws securing the vessel lid to the vessel body were removed. After removal, the vessel lid was separated from the vessel body. Separating the vessel liner from the vessel lid was challenging (Figure 12B). The vessel lid and the vessel liner were separated by first loosening the Swagelok nuts securing the thermowell (P3) and the sparge tube (P4). Then, lightly tapping both the thermowell and the sparge tube with a box wrench allowed the vessel lid to slide off. Images of the underside of the vessel lid (Figure 12C) and the vessel liner (Figure 12) were captured.

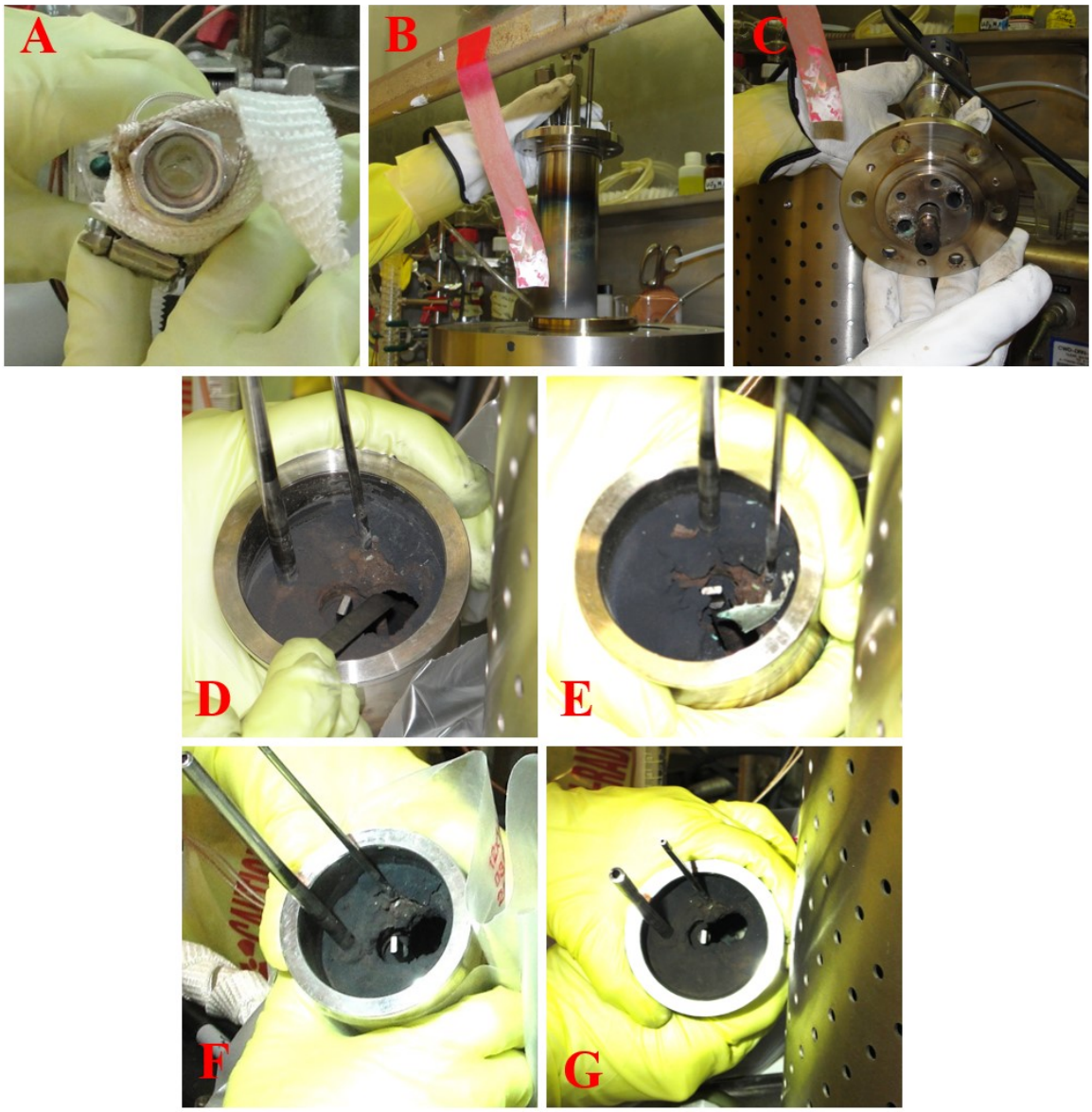

Figure 12. A) View down the quartz salt condenser. B) Vessel lid and vessel liner after cooling. C) Underside of vessel lid. D-G) View of the vessel liner after cooling.

2.4 Experiment 2: HCl Flow Rate on UO_2 Hydrochlorination

The procedure for Experiment 2 was performed according to Section 2.2 with the following exceptions mentioned here.

A reaction mixture of NaCl, CsCl, and UO_2 was prepared with the masses listed in Table A 1. All three solids were well-mixed and added to the reaction vessel liner through the sampling port. An air-tight seal between the vessel lid and the reaction vessel liner was created using one Hastelloy gasket flanked by two aluminum oxide fiber gaskets. This combination of gaskets was utilized for Experiments 2-5.

Once the contents of the vessel liner temperature stabilized at 650 °C, the HCl gas flow rate was set according to Table 2. Similar to Experiment 1, there was no evidence that the impellor was stirring the reaction mixture throughout the experiment. Rhythmic tapping of the impellor along the vessel line was not

audible and dipping the Hastelloy rod into the path of the impellor did not result in the impression that the impellor was striking the rod. Samples were collected every thirty minutes by inserting the threaded Hastelloy rod through the sampling port. The collected solids were bright blue in color and appeared like those collected in Experiment 1. These solids were added to pre-weighed centrifuge tubes with water, and then the mixtures were reweighed again. The mixture had dark precipitates suspended within a green solution (Figure 13). These samples were filtered, acidified, and analyzed via UV-vis spectroscopy per the general experimental conditions discussed. Over time, the intensity of the solution's green color appeared to decrease. Water masses and dip sample masses were tabulated in Table A 2.

Table 2. Timeframe and the corresponding HCl gas flow rates for Experiment 2.

Timeframe (h)	HCl flow rate (mL/min)
0-2	200
2-4	330
4-5	480

Figure 13. Filtered and acidified dip sample.

As the hydrochlorination progressed, condensation and a thin film of yellow solids was observed at the inlet of the water condenser (Figure 14A). The condensation appeared to displace some of the yellow solids and both the condensate and dissolved solids were collected in the graduated cylinder (Figure 14B). The volume collected in the graduated cylinder was recorded at the same time when the dip sample was collected.

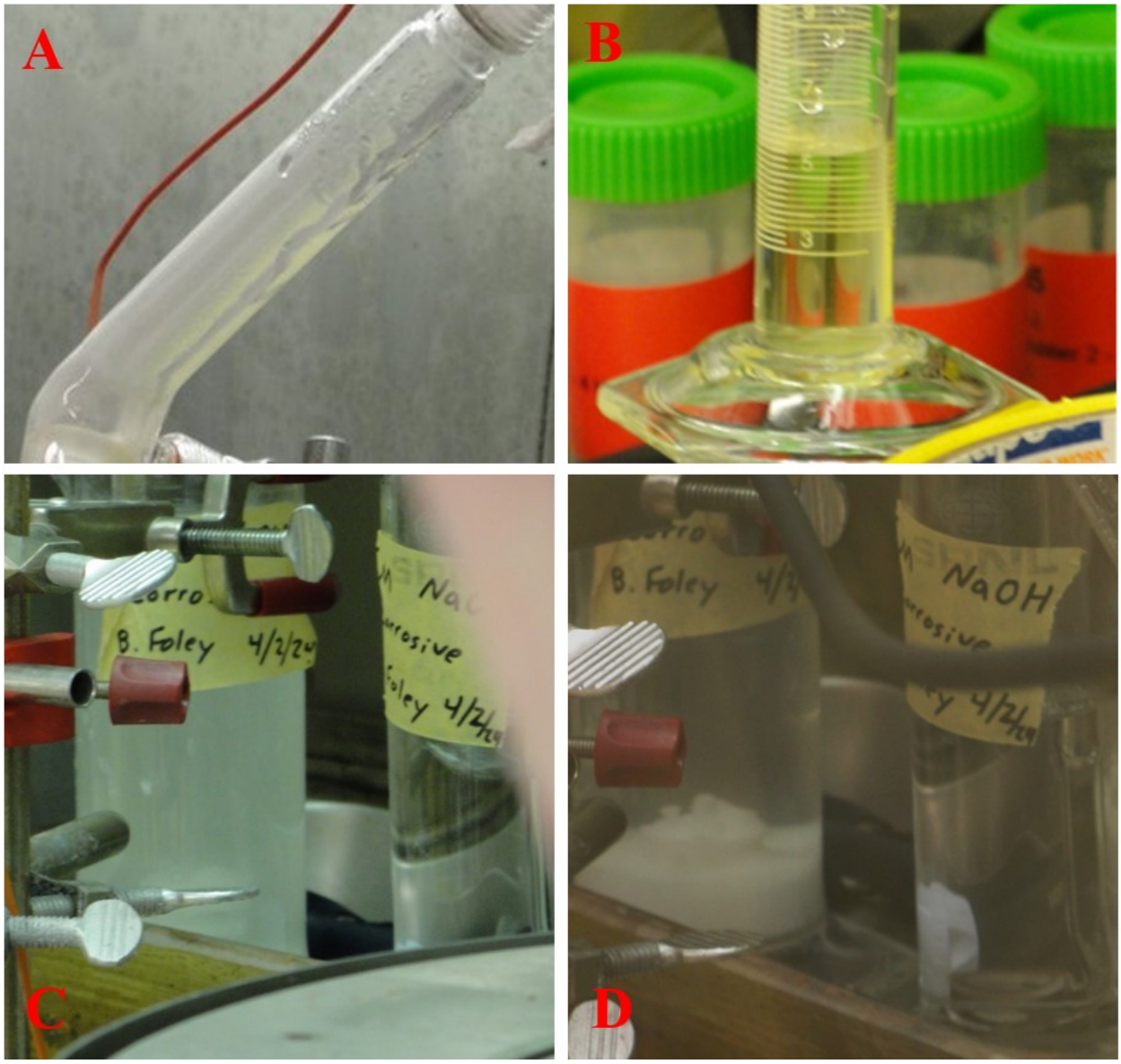

Figure 14. A) Yellow solids at the inlet of the water condenser. B) Condensate collected in the graduated cylinder. C) Contents of scrubber bottle 1 becoming cloudier. D) White crystals stemming from the frit of scrubber bottle 1 and white precipitates settled at the bottom of the bottle.

At the 2-, 4-, and 5-hour timepoints, 15 mL aliquots of both scrubber bottles were collected for analysis. Scrubber bottle 1 samples were analyzed via neutron activation analysis (NAA), Ion Chromatography-Anions (IC-Anions), and Inductively Coupled Plasma Mass Spectrometry (ICP-MS). Scrubber bottle 2 samples were analyzed by NAA. As time progressed, scrubber bottle 1 became noticeably cloudier with white solids (Figure 14C and D). Towards the end of the experiment, scrubber bottle 1 had a growth of white crystals stemming from the frit. Scrubber bottle 2 had a visibly larger hole in the center of the frit, which resulted in fewer, but larger bubbles. The growth of the crystals on the frit prompted a decision to stop the experiment after 5 h instead of the planned 6 h.

After the apparatus cooled, disassembly revealed a small film of yellow solids along the quartz salt condenser (Figure 15A). The underside of the vessel lid had blue solids along various ports, likely indicating

corrosion (Figure 15B). Furthermore, the contents of the reaction vessel liner appeared as a blue/black solid (Figure 15C, D, and E).

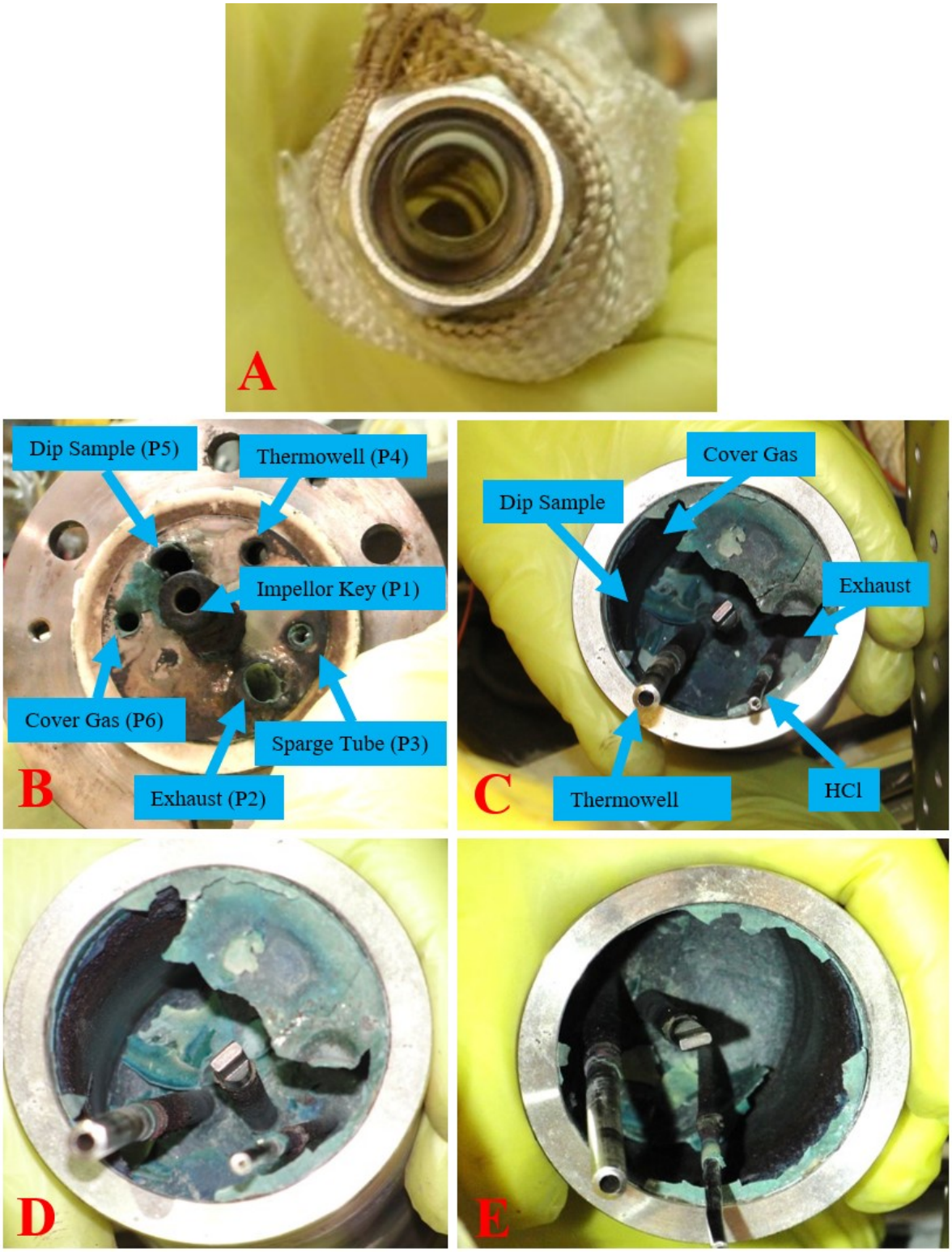

Figure 15. A) View down the quartz salt condenser from Experiment 2. B) Underside of the vessel lid. C-E) Contents of the vessel liner.

2.5 Experiment 3: Thermodynamic Analysis of UO_2 Hydrochlorination

The procedure for Experiment 3 was performed according to Section 2.2 with the following exceptions mentioned below.

Based on observations made during Experiment 2, the inability of the impellor to stir was hypothesized to be caused by the large quantity of UO_2. The UO_2 would settle as a solid in the reaction vessel liner and may have prevented stirring. A second hypothesis involved insufficient cooling from air to the magnetic stirrer coupling and that water-cooling may have been necessary to protect the magnetic coupling. To address these issues and to promote stirring, the following changes were incorporated.

The entire apparatus was assembled, and the magnetic stirrer was set to rotate the impellor at 280 rpm. A rhythmic noise suggested the impellor was rotating, but this noise was inconsistent and would be inaudible for periods of time before becoming audible again. The empty reaction vessel liner was then heated to 650 °C. The masses (Table A 1) of NaCl and CsCl were well-mixed and slowly added to the reaction vessel in a piece-wise fashion. The salt addition was performed with a custom glass funnel. Slow addition of the eutectic mixture was done to prevent a large mass of solid from inhibiting the stirrer while allowing the added eutectic mixture to melt. After adding the eutectic salt mixture, the UO_2 was added. A smaller quantity of UO_2 was selected to minimize resistance against the rotation of the impellor while assessing whether complete hydrochlorination could be achieved.

Despite the slow addition of salt and smaller quantity of UO_2, the impellor was not stirring. Though the magnetic coupler was not air-cooled for this experiment, the temperature of the magnetic coupler was checked periodically and was determined to not exceed 33 °C, suggesting temperature control of the magnetic coupler may not have been problematic. One possible explanation was that the magnetic couple required a particularly strict alignment with the stir shaft to function properly and was not achievable due to a weak magnetic coupling. Due to these challenges, stirring the reaction mixture was not attempted for this experiment or further experiments.

Experiment 3 occurred over two non-sequential days with a week in between. An HCl flow rate of 260 mL/min was utilized for both days. Day one involved six hours of HCl flow with sampling every 30 minutes. Scrubber bottle 1 and 2 had 300 mL and 200 mL of 5 M NaOH solution, respectively. A new bottle with an intact frit was used for scrubber bottle 2 for Experiments 3-5. At the 2-, 4-, and 6-h timepoints, 5.5 mL aliquots of both scrubber solutions were collected for IC-Anions analysis. A sample of the molten salt mixture was collected at the 6-h timepoint for pXRD analysis.

After 6 h, the sparge tube was carefully retracted from the surface of the molten salt mixture and the experimental apparatus was cooled under an argon flow of 50 mL/min. Scrubber bottle 1 was cloudy with white precipitates. Both solutions in the scrubber bottles were replaced prior to the second day of hydrochlorination. After one week at room temperature, day two of the hydrochlorination began by reheating the apparatus to 650 °C. Once heated to 650 °C, a sample was collected for UV-vis analysis. The sparge tube was reinserted into the reaction vessel liner and HCl flow was initiated. Samples were collected every hour for six hours and analyzed by UV-vis spectroscopy and ICP-MS analysis. The masses of the dip samples were tabulated in Table A 2. The scrubber solutions were not analyzed for day two of the hydrochlorinations.

2.6 Experiment 4: UO_2 Hydrochlorination in the Presence of Fissium

The procedure for Experiment 4 was performed according to Section 2.2 with the following exceptions mentioned below.

The masses of NaCl, CsCl, and UO_2 listed in Table A 1 were well-mixed and added to the reaction vessel liner. Notably, for this experiment, the reaction vessel liner was heated to 650 °C prior and the sample was allowed to cool. On a separate day, this previously melted mixture was reheated to 650 °C. The remaining compounds, a mixture of fission product simulants referred to as Fissium, are listed in Table A 1. These compounds were selected to simulate a Fissium content[5,6] that was 5% by weight of the uranium mass. This mixture was added to the reaction vessel liner through the sampling port.

Hydrochlorination occurred at a HCl gas flow rate of 260 mL/min for six hours. Samples were collected at every hour timepoint. Collected sample masses were listed in Table A 2. For the scrubber solutions, 200 mL and 300 mL of 5 M NaOH solutions were used for scrubber bottle 1 and scrubber bottle 2, respectively. At the 2, 4, and 6 h timepoints, a 15 mL aliquot from both scrubber bottles were collected and analyzed for IC-Anions. A pXRD sample was collected at the 6 h timepoint.

On the following day, the experimental apparatus was disassembled. The inlet to the salt condenser (P2), salt condenser, and outlet of the salt condenser/inlet of the water condenser were rinsed with aliquots of dilute HNO_3 (Figure 16). All three rinses were submitted for ICP-MS. Upon disassembly, the HCl sparge tube appeared to be broken or corroded (Figure 17). The sparge tube was shorter in length than before the hydrochlorination experiment and only extended down to the surface of the solidified reaction mixture. Presumably, the remaining length of the sparge tube was broken off and remained submerged in the solidified reaction mixture. It is unknown if the HCl gas was sparged through the salt throughout the duration of the experiment. The broken tube was believed to be partially submerged below the molten salt. Discoloration (darker) on the lower portions of the broken sparge tube suggested that a segment of the sparge tube was submerged below the molten salt. An increase in molten salt volume when heated allowed for greater submersion of the sparge tube. In contrast, a decrease in molten salt volume when cooling brought the molten salt volume below the opening of the sparge tube.

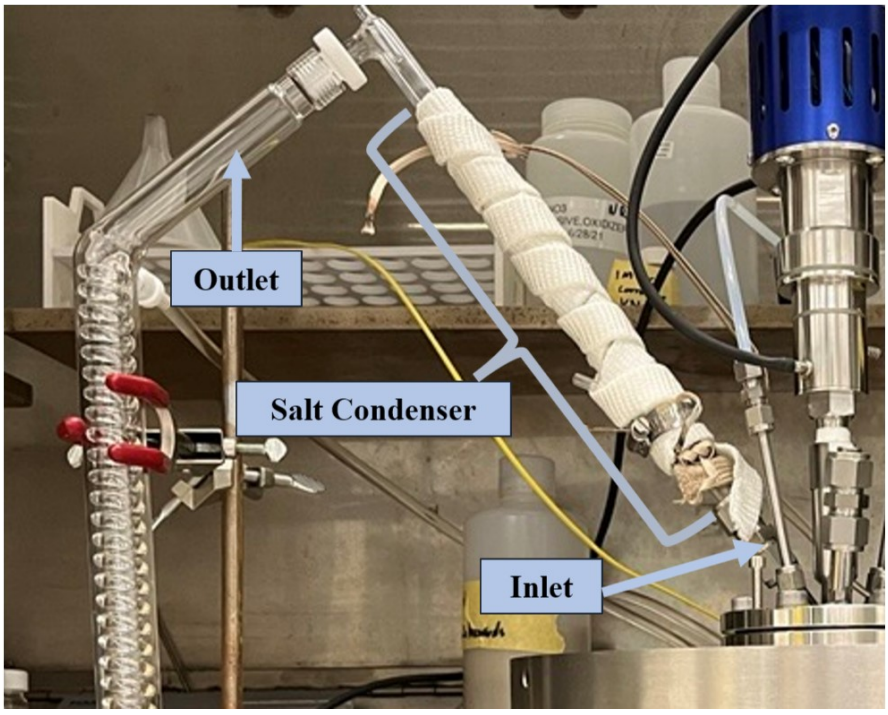

Figure 16. Salt condenser inlet, salt condenser, and outlet of the salt condenser (or inlet of the water condenser) that was rinsed for analysis.

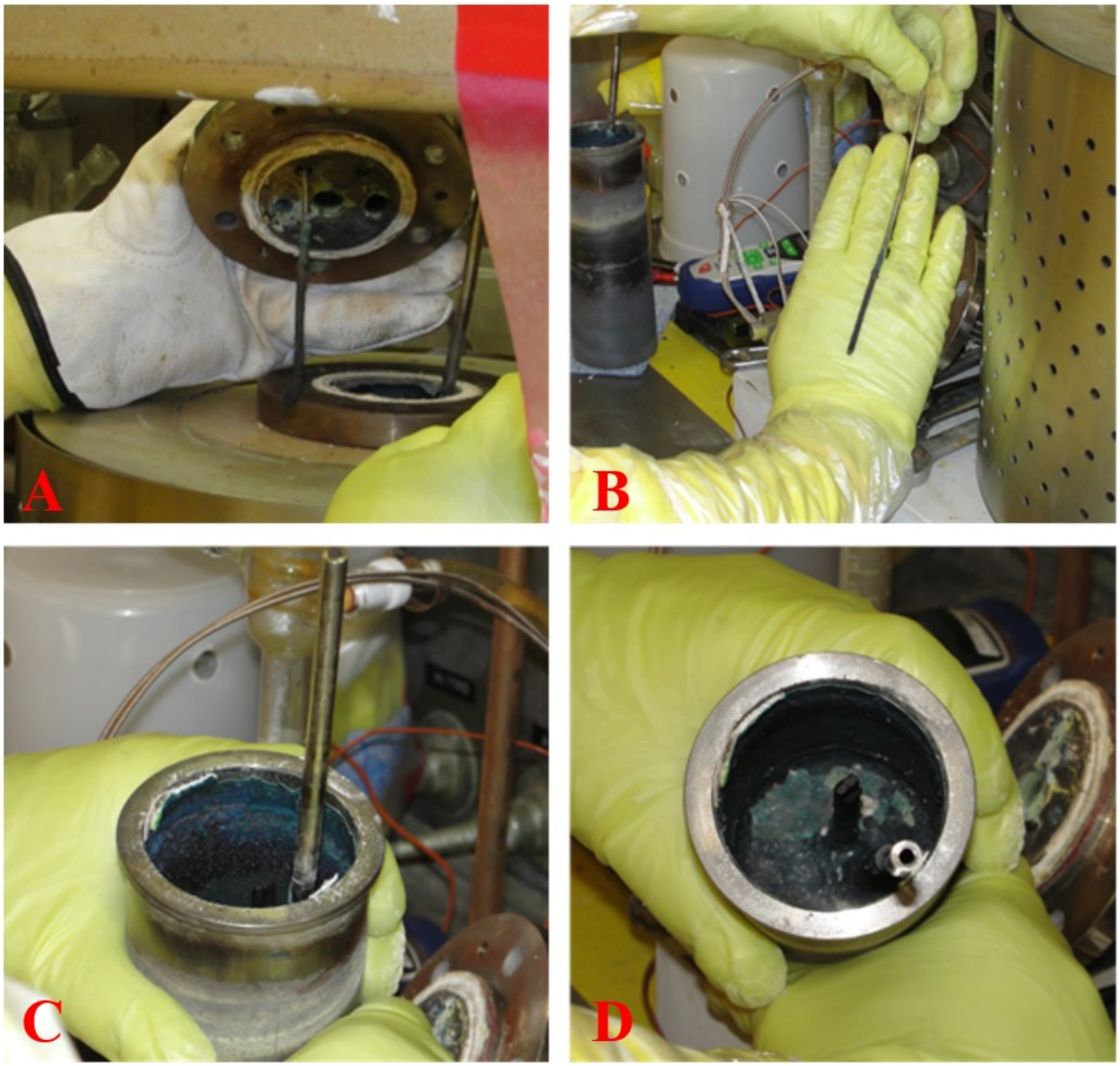

Figure 17. A) Underside of the vessel lid. B) Upper portion of broken sparge tube. C-D) Vessel liner contents.

2.7 Experiment 5: Frit Sparger Improvement for Increased HCl Contact

The procedure for Experiment 5 was performed according to Section 2.2 with the following exceptions mentioned below.

To encourage a greater degree of hydrochlorination, an alternative sparger design was implemented (Figure 18) to promote HCl gas and UO_2 contact. This alternative design was a Hastelloy C276 cup equipped with a 40 µm pore size frit towards the bottom of the cup. A ⅛ in. Hastelloy C276 tube passed through the frit. The design was for the solid UO_2 to be added on top of the frit allowing HCl gas to be introduced below the frit and sparged through the frit as bubbles. This alternative sparger design replaced the ⅛ in. Hastelloy C276 tube that was extending through the port, P4. The masses, listed Table A 1, were well-mixed to target a UO_2 solid that was incorporated with the NaCl-CsCl salt mixture. After this blend was added to the

Hastelloy cup, the experimental apparatus was setup with the Hastelloy C276 cup in lieu of the ⅛ in. sparge tube. Additional NaCl and CsCl were added through the sampling port to reach the masses listed in Table A 1. Hydrochlorination proceeded for six hours and samples were collected every 45 minutes. A 5-mL aliquot was collected from each scrubber bottle every 1.5 hours and analyzed via IC-Anions and ICP-MS. It should be noted that white precipitates appeared shortly after the 3-h timepoint for scrubber bottle 1. For the remaining 3 h, scrubber bottle 1 was bypassed and only scrubber bottle 2 was used. A pXRD sample was collected at the 6 h timepoint.

Figure 18. Gas sparger design for Experiment 5 showing the frit sparger and reaction vessel liner.

2.8 Quality Assurance

Requirements for performing reviews of technical reports and the extent of review are established in manual E7 2.60. SRNL documents the extent and type of review using the SRNL Technical Report Design Checklist contained in WSRC-IM-2002-00011, Rev. 2.

3.0 Results and Discussion

3.1 Molten Salt Mixture

3.1.1 ICP-MS Analysis

ICP-MS concentrations for U-235 and U-238 are listed in Table A 3. Total U concentrations were calculated (Equation A1) using the measured U-235 and U-238 concentrations that were above the limit of detection (LOD). The U-235 and U-238 concentrations for timepoints 1-5 h for Experiment 1 were below LOD (100 µg/L).

Given the dip samples were suspended in water and filtered, undissolved solids were removed, and the resulting solution should only have water soluble U species present. The ICP-MS samples were made by acidifying the solutions with HNO_3, which also diluted the overall water-soluble U concentration. The water-soluble U concentration of the suspended dip samples was back-calculated using Equation 2 and Equation 3 to account for acidifying the filtered dip sample solution. The total U concentrations (Table A 3) were utilized for these calculations. Equation 4 was used to calculate the mass of water-soluble U on the dip sample. The volume of water for each sample was obtained by assuming a water density of 1 g/mL for the masses listed in the following tables: Table A 2. The mass of water-soluble U in the reaction vessel was calculated (Equation 5) using the total mass of reaction mixture (Table A 1) and the dip sample weight (Table A 2). Equation 6 was used to calculate the percent conversion of UO_2 to a water-soluble U species. The starting moles of UO_2 (or U) was obtained from Table A 1. The calculated values were tabulated in Table 3.

Table 3. Water-soluble U content and percent conversion.

Experiment 1: Uranium Salt Bridge				
Timepoint (h)	Water soluble U conc. (g/L)	Mass of water soluble U in dip sample (g)	Mass of water soluble U in reaction vessel (g)	% conversion
6	3.95×10^{-4}	7.90×10^{-6}	1.29×10^{-3}	3.66×10^{-4}
Experiment 2: HCl Flow Rate on UO_2 Conversion				
Timepoint (h)	Water soluble U conc. (g/L)	Mass of water soluble U in dip sample (g)	Mass of water soluble U in reaction vessel (g)	% conversion
1	7.57×10^{-1}	1.46×10^{-2}	12.8	3.6
2	1.67	3.21×10^{-2}	23.9	6.7
3	3.23	6.25×10^{-2}	43.7	12.3
4	2.95	5.63×10^{-2}	78.1	21.9
5	5.47	1.05×10^{-1}	82.1	23.0
Experiment 3: Thermodynamic Analysis of UO_2 Hydrochlorination				
Timepoint (h)	Water soluble U conc. (g/L)	Mass of water soluble U in dip sample (g)	Mass of water soluble U in reaction vessel (g)	% conversion
1	0.074	1.45×10^{-3}	0.40	0.8
2	0.204	4.08×10^{-3}	1.60	3.2
3	0.373	7.46×10^{-3}	2.86	5.8
4	0.452	9.03×10^{-3}	4.04	8.2
5	0.538	1.07×10^{-2}	5.35	10.8
6	0.570	1.14×10^{-2}	5.86	11.9
7	0.706	1.42×10^{-2}	7.66	15.5
8	0.758	1.53×10^{-2}	8.59	17.4
9	0.956	1.92×10^{-2}	10.64	21.6
10	1.211	2.44×10^{-2}	11.08	22.4
11	1.046	2.11×10^{-2}	9.44	19.1
12	0.249	4.99×10^{-3}	8.42	17.1

Experiment 4: UO_2 Conversion in the Presence of Fissium				
Timepoint (h)	Water soluble U conc. (g/L)	Mass of water soluble U in dip sample (g)	Mass of water soluble U in reaction vessel (g)	% conversion
1	2.46×10^{-3}	4.92×10^{-5}	2.85×10^{-3}	8.0×10^{-3}
2	*	*	*	*
3	0.197	3.94×10^{-3}	2.23	0.6
4	0.878	1.75×10^{-2}	10.92	3.1
5	0.542	1.08×10^{-2}	8.13	2.3
6	0.819	1.64×10^{-2}	10.20	2.9
Experiment 5: Frit Sparger Improvement for Increased HCl Contact				
Timepoint (h)	Water soluble U conc. (g/L)	Mass of water soluble U in dip sample (g)	Mass of water soluble U in reaction vessel (g)	% conversion
0.75	0.201	4.03×10^{-3}	1.35	1.5
1.5	0.358	7.13×10^{-3}	2.46	2.8
2.25	0.411	8.18×10^{-3}	4.09	4.6
3	0.596	1.19×10^{-2}	4.38	4.9
3.75	0.504	1.00×10^{-2}	5.07	5.7
4.5	0.680	1.36×10^{-2}	4.82	5.4
5.25	0.603	1.21×10^{-2}	5.91	6.6
6	0.590	1.18×10^{-2}	6.08	6.8

*Measured ICP-MS concentrations were below LOD.

$$Water\ soluble\ U\ conc.\left(\frac{g}{L}\right) = Total\ U\left(\frac{\mu g}{L}\right) \times \frac{1\ g}{1\times10^{6}\ \mu g} \times Dilution\ \text{Factor} \qquad \text{Equation 2}$$

$$Dilution\ Factor = \frac{5\ mL\ acified\ solution}{4.5\ mL\ filtered\ solution} = 1.11 \qquad \text{Equation 3}$$

$$Mass\ of\ water\ soluble\ U\ in\ dip\ sample\ (g) = Water\ soluble\ U\ concentration\ \left(\frac{\text{g}}{\text{L}}\right) \times Volume\ of\ water\ (\text{L}) \qquad \text{Equation 4}$$

$$Mass\ of\ water\ soluble\ U\ in\ reaction\ vessel\ (g) = Mass\ of\ water\ soluble\ U\ in\ dip\ sample \times \frac{Mass\ of\ reaction\ mixture\ (g)}{Dip\ sample\ weight\ (g)} \qquad \text{Equation 5}$$

$$\%\ conversion = \left(Water\ soluble\ U\ in\ dip\ sample\ (\text{g}) \times \frac{Mol\ U}{Atomic\ Mass\ U238\ (g)} \times \frac{Mol\ UO_2}{Mol\ U}\right) \div Starting\ mol\ UO_2 \times 100\% \qquad \text{Equation 6}$$

The percent conversion obtained during Experiment 1 indicated hydrochlorination did not occur. Observations of the vessel liner revealed a top layer that matched the description of uranium oxides and a

bottom layer that appeared to be a solidified mix of NaCl/CsCl. A likely explanation would be the eutectic salt mixture became less dense when melted. This would cause the NaCl/CsCl mixture volume to decrease. Since the UO_2 was added to the vessel liner after the NaCl/CsCl mixture, the UO_2 powder likely remained as a top layer with a gap between the UO_2 and NaCl/CsCl once the NaCl/CsCl layer retracted during melting.

The percent conversion for Experiments 2 and 3 indicated hydrochlorination could be achieved (Figure 19). Both of these experiments had maximum percent conversions around 22-23%, which was similar to the Phase 1 experiment performed at 650 °C.[4] For Experiment 2, various HCl flow rates were assessed between timepoints 0-2 h (200 mL/min), 2-4 h (330 mL/min), and 4-5 h (480 mL/min). The overall percent conversion increases after each hour. However, the percent conversion only increases by 1.1% between the 4-h and 5-h timepoint, which was significantly less than the change between the previous timepoints. The percent conversions achieved at each flow rate suggested higher HCl flow rates resulted in higher percent conversions, but the return on percent conversion was less pronounced after a certain HCl flow rate. This conclusion could be made from just the Experiment 2 results; however, Experiments 3 and 4 would suggest other factors were influential.

For Experiment 3, the percent conversion increased throughout the experiment until the 10-h timepoint and then decreased after the 10-h timepoint. After reaching a maximum of 22.2%, the percent conversion decreased to 18.9% and 16.8% at the 11-h and 12-h timepoints, respectively. Though the inhomogeneity of the dip sample and the reaction mixture could contribute to sampling inconsistencies, the percent conversions at the 11-h and 12-h timepoints were the only timepoints to deviate from an increasing trend. Rather than associating the decrease in percent conversion to the sampling variations, the sample-to-sample consistency indicate that the decrease in water-soluble U species could be due to volatilization or undesired side reactions.

The desired product, UCl_4, is more readily volatile than the other reaction mixture components.[7] At elevated temperatures, UCl_4 could exit the reaction mixture and condense within the off-gas system (salt condenser, water condenser, scrubber solutions, etc.). Though the molten salt could suppress UCl_4 volatilization, literature reports have indicated greater volatilization as the dissolved UCl_4 concentration increases.[7] Small amounts of yellow solids could be observed along the salt condenser (Figure 16), water condenser, and tubing in the off-gas system. Given, UO_2Cl_2 could be eventually formed by the oxidation or hydrolysis of UCl_4, the yellow solids could be due to volatilized water-soluble U species. Loss of water-soluble U species from the vessel liner would contribute to a decrease in the calculated percent conversion.

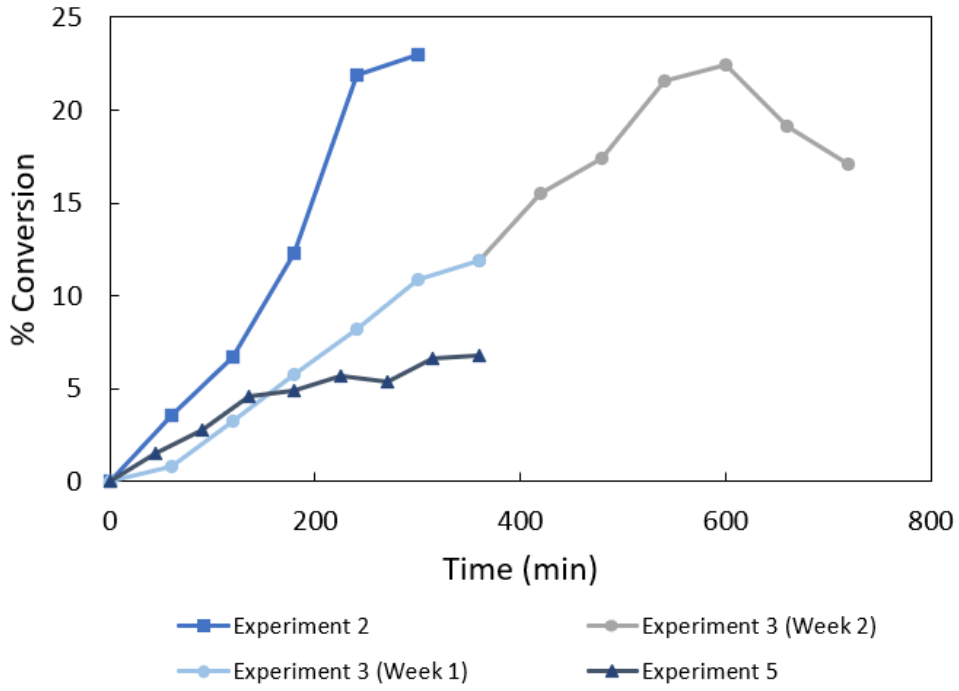

Figure 19. Percentage of conversion of soluble uranium species at 650 °C during hydrochlorination. Results from tests varying condition parameters are shown.

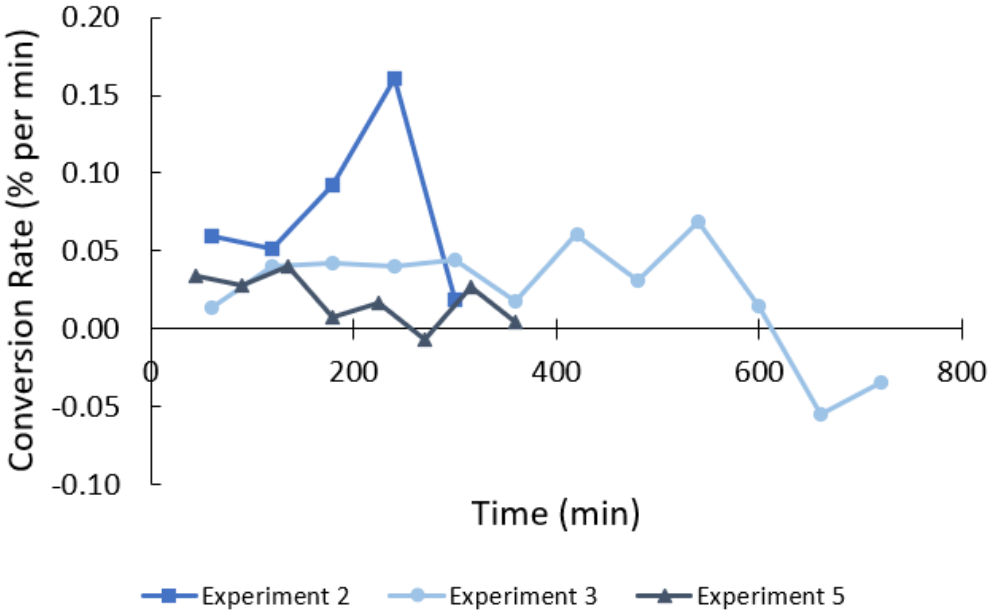

Figure 20. Rate of percentage of conversion of soluble uranium species at 650 °C during hydrochlorination. Results from tests with varying condition parameters are shown.

Successful hydrochlorination, per Equation 1, should generate water as a byproduct. Water can hydrolyze UCl_4 to generate intermediates, such as uranium hydroxides and $UOCl_2$, which can further hydrolyze to form uranium oxide.[8-11] Furthermore, the desired product, UCl_4, can comproportionate with unreacted starting material, UO_2, to generate two equivalents of $UOCl_2$.[12] In the presence of chlorides and oxygen, UO_2 and $UOCl_2$ can oxidize to form UO_2Cl_2.[11] At elevated temperatures, UO_2Cl_2 slowly decomposes to form uranium oxides and chlorine gas.[13] And as previous established by Volkovich, hydrochlorination of

UCl_4 may form UO_2Cl_2 as an impurity.[3] At 650 °C, NaCl-CsCl molten salt media promoted UCl_4 formation while minimizing UO_2Cl_2; however, the variety of conditions used by Volkovich highlights the sensitivity of the reaction towards temperature and salt matrix. Regardless, successful UO_2 hydrochlorination produces water, which cannibalizes the desired product. Despite the elevated temperature of the reaction vessel, enough water was present in the reaction vessel to inhibit efficient UCl_4 formation.

Due to the insolubility of uranium oxides, these UCl_4 and UO_2Cl_2 decomposition pathways would decrease the water-soluble U species concentration and, thus, the percent conversion. These aforementioned reasons could all contribute to a larger decrease in percent conversion.

In Experiment 4, percent conversion reached a maximum of 3.1%, and the subsequent timepoints at 5-h and 6-h were lower than 3.1%. An overall lower percent conversion was likely seen for Experiment 4 due to the broken sparge tube. A truncated sparge tube would have less depth and the sparged HCl would be less effectively dispersed throughout the molten salt. Contact between then UO_2 settled at the bottom of the vessel liner and the HCl sparged into the top of the molten salt mixture would be less than that of Experiment 2 or 3. Due to a broken sparge tube, it is inconclusive on the role that the fissium elements played. More studies would have to be done to determine if the fissium reagents influenced overall UO_2 conversion.

Experiment 5 utilized the frit sparger to increase reagent contact. Though this design increased contact between UO_2 and HCl, the maximum percent conversion calculated was only 6.8%. While UO_2 and HCl contact increased, the contact between the products, UCl_4 and water, would also increase. So, while product formation could be higher, the decomposition rate of the products could also increase.

In Figure 20, an analysis of the percent conversion rate during hydrochlorination indicated Experiment 2 had a slightly greater rate of hydrochlorination. Notably, the rate of hydrochlorination appeared to increase in Experiment 2 when the HCl flow rate was increased. However, this rate decreased and the percent conversion appeared to level off towards the 5-h timepoint. Similarly, the percent conversion for Experiment 3 reached a maximum at the 10-h timepoint and began to decrease. Though the rate of hydrochlorination for Experiment 5 did decrease over time, the percent conversion (Figure 19) did not appear to hit a maximum before decreasing. However, this may be obscured due to the limited timepoints analyzed.

Another factor that could influence hydrochlorination of UO_2 was the corrosion products. Likely, the blue solids observed on the underside of the vessel lid was due to corrosion. Detailed elemental analyses were collected at particular timepoints and summarized (Table A 4-Table A 6) for Experiments 3-5 to assess for corrosion-related elements. For Experiment 3, transition metals often found in Hastelloy C276 were detected (Table A 4), such as Ni, Cr, Fe, Mn, Co, and Mo. The vessel lid was reused for all five experiments; therefore, Experiments 4 and 5 also contained various elements associated with Hastelloy C276 corrosion that appeared to generally increase in concentration as hydrochlorination progressed (Table A 5 and Table A 6). Though W was not measured in Experiments 3 and 4, W was detected in samples taken from Experiment 5, which is another common element found in Hastelloy C276.

For Experiment 4, the Fissium elements (Mo, Pd, Re, Rh, Ru, and Zr) were measured. The measured change in Ru and Re concentrations appeared inconsistent, with concentrations appearing on the cusp of the instrument's LOD. The concentrations of Pd, Rh, and Zr were below the LOD; however, these elements were only present in small quantities at the start. Due to the broken sparge tube preventing an effective HCl sparge through the reaction mixture, the effect of the Fissium elements on the hydrochlorination of UO_2 could not be well-assessed.

For Experiment 5, the change in concentration for elements found soluble in the dip sample can be visualized in Figure 21. Normalized concentrations were determined by taking the measured element

concentration and dividing by the dip sample mass (Table A 7). As hydrochlorination progressed, the concentrations of Cr, Mn, Fe, Co, and Ni increased. Notably, the water-soluble Ni concentration drastically increased and surpassed the normalized concentration of water-soluble U. If the concentration of insoluble Rb, Mo, and W related compounds increased, the values would not be encompassed in this dataset. Therefore, the concentrations of Rb, Mo, and W remained relatively consistent, especially in comparison to Ni.

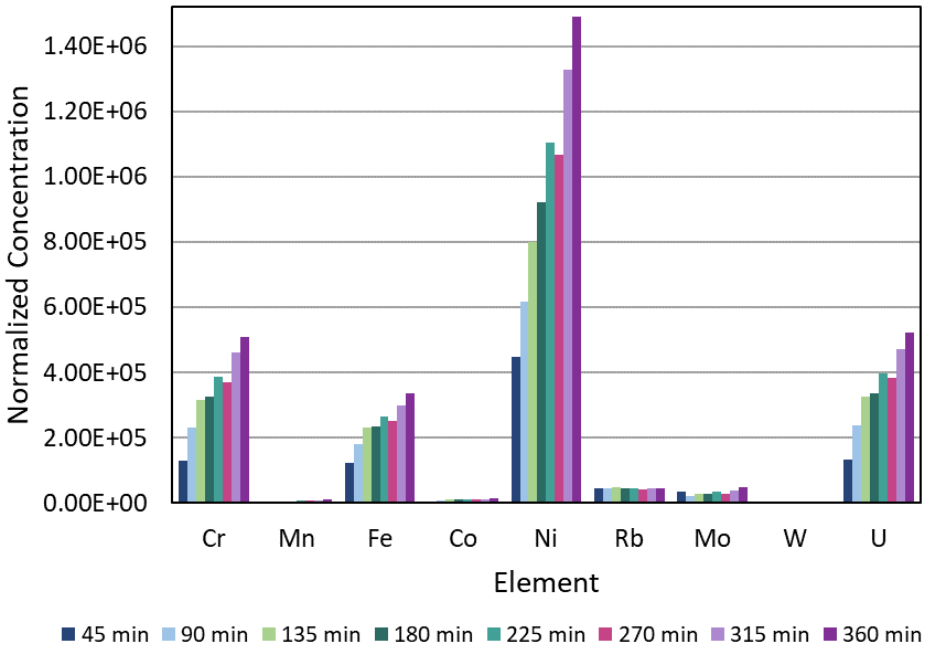

Figure 21. Normalized concentrations of elements found in dip samples during Experiment 5.

Despite the touted acidic resistance of Hastelloy C276, the material is susceptible to corrosion. In particular, oxygen and water could hasten the rate of corrosion. While reactions in molten salts would ideally utilize inert gloveboxes to exclude air and humidity or molten salt loops to prepare high purity anhydrous salts, the hydrochlorination reaction examined in this report generates a problematic byproduct. Successful hydrochlorination of UO_2 generates two equivalents of water, which would accelerate corrosion of the reaction vessel. For reaction vessels that are intended for long-term or repeated use, such as an industrial-scale system, the corrosive effect caused by water can begin to compound and compromise the integrity of the system. For Experiments 1-5, inert gloveboxes and rigorously purified salts were not available or utilized; however, even if Experiments 1-5 were performed with these reagents and conditions, the water byproduct presents an ongoing issue. The imperfect conditions in Experiments 1-5 advantageously highlights the sensitivity of the system to non-inert atmospheric conditions and the corrosion-related challenges of the system.

3.1.2 UV-vis Spectroscopy Analysis

The 1 M HNO_3 solutions prepared from the dip samples were analyzed via UV-vis spectroscopy. Based on literature values for 1 M HNO_3 solutions, the wavelengths used to quantitate U(IV) and U(VI) species were 414.3 nm and 647.4 nm, respectively.[14,15] The molar absorptivities for U(IV) and U(VI) were determined using Sinkov's report.[14] UV-vis data was utilized to quantitate the total U and differentiate between U(IV) and U(VI). Though UV-vis samples from Experiment 2 had absorbances at wavelengths associated with U(IV)/U(VI) species that were similar to Phase 1 spectra (Figure 22), quantifying the results indicated a percent conversion much greater than 100%. Thus, suggesting the results were unreliable. Furthermore, the

UV-vis spectra baseline became unreliably noisy and populated with unidentified peaks that were not consistent between timepoints. This observation became more apparent during later experiments.

Several factors complicated the UV-vis data. The dip samples and many of the UV-vis solutions were notably blue. Blue was not an expected color for U(IV) or U(VI) species, which were expected to be green or yellow, respectively. Given blue solids were observed on the Hastelloy C276 vessel and were likely corrosion products, these solids could contain soluble species that adsorb at wavelengths overlapping with U(IV) and U(VI) species. Overlapping absorbances at 414.3 nm and 647.4 nm would contribute to the absorbance value used to determine the U(IV) and U(VI) concentrations; thus, inflating those calculated concentrations. Furthermore, the presence of numerous potential corrosion products conflated the UV-vis data. As a result, the concentrations calculated by UV-vis would not be reliable for the current system.

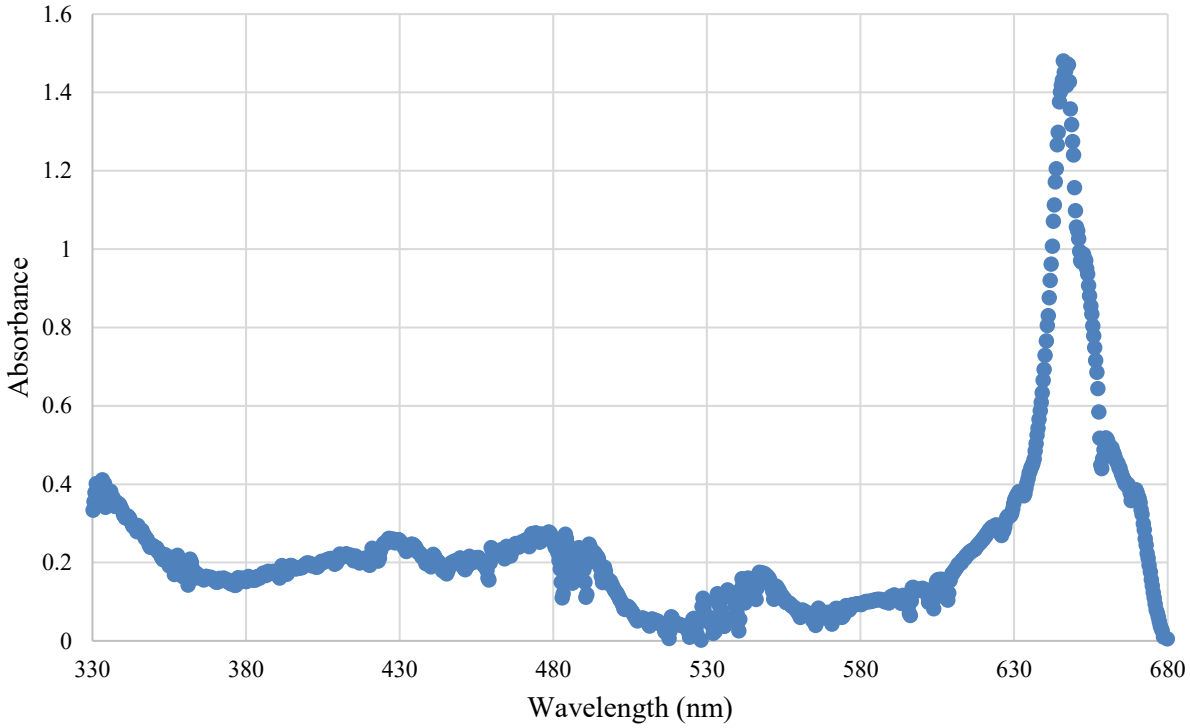

Figure 22. Example UV-vis spectrum from Experiment 2 at the 5-h timepoint.

3.1.3 Powder XRD Analysis

For each experiment, a sample was collected for pXRD analysis, which enabled the measurement of solid samples. Powder XRD results (Figure 23) showed the presence of few water-soluble (NaCl, CsCl, $CsNiCl_3$) and insoluble compounds (UO_2). These results are not consistent with the ICP-MS analyses in which water-soluble U complexes were seen. However, due to the limit of detection of pXRD (0.5 wt%), these compounds are not an exhaustive list of all complexed formed. The analysis was also done on a room temperature sample from the molten salt and the measurements were not taken in-situ at temperature. Therefore, the complexes fitted are a best fit based on what is seen through ICP-MS and UV-vis analyses. Notably, species suggesting successful hydrochlorination, such as UCl_4 or $Cs_2UO_2Cl_2$, were not detected, which contrasts with the Phase 1 experiments.

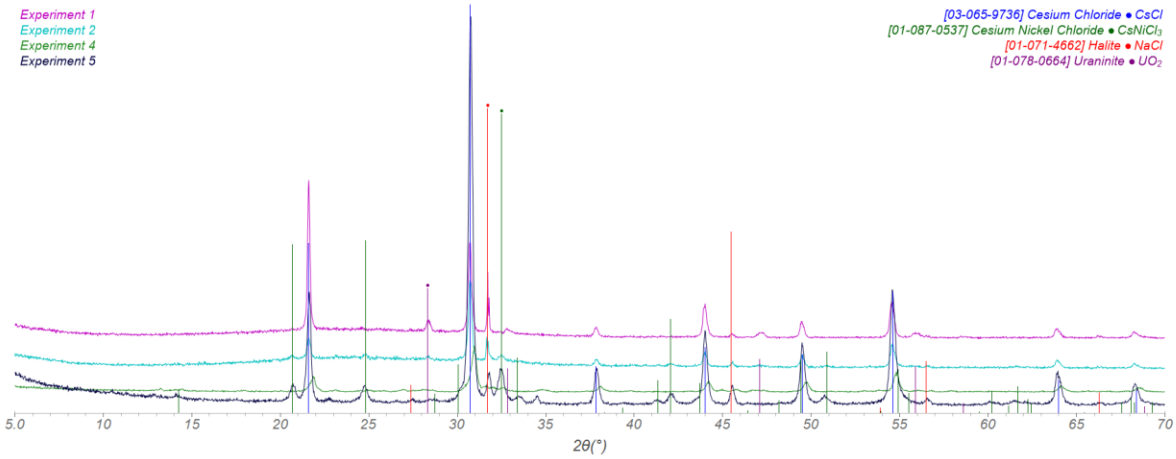

Figure 23. pXRD results from Experiments 1-5.

3.2 Salt Condenser

During the disassembly of the Experiment 4 apparatus, rinses from the salt condenser, salt condenser inlet (inlet), and salt condenser outlet (outlet), see Figure 16, were analyzed by ICP-MS (Table 4). The total U content decreased moving away from the reaction vessel liner from the inlet (2.76×10^5 µg/L) to the salt condenser (6.55×10^3 µg/L) and then to the outlet (7.92×10^3 µg/L). Likewise, the other elements decreased in concentration moving away from the reaction vessel liner, with the exception of Cr and Mn. The elements, Cr, Mn, and Fe had lower concentrations on the condenser than the inlet and outlet. Rinse concentrations of Co, Zr, Ru, Rh, Pd, and Re were all below the LOD for all three rinses. The most abundant elements were Cr, Fe, Ni, and Mo, which were all elements present in Hastelloy C276. At the condenser inlet was Rb, which had concentration of 6.20×10^3 µg/L. Besides Mo, Rb was the only other fissium element detected within the inlet, condenser and outlet. Given the yellow coloration of Ni chloride species, the yellow solids present in the off-gas system could be due to Ni chlorides and/or U(VI) species.

Table 4. ICP-MS concentrations (µg/L) from the rinses from the salt condenser inlet, salt condenser, and the outlet of the salt condenser for Experiment 4.[#]

Element/Isotope	Condenser Inlet	Condenser	Condenser Outlet
U-235	**	**	**
U-238	2.76×10^5	6.55×10^3	7.92×10^3
Total U	2.76×10^5	6.55×10^3	7.92×10^3
Cr	8.38×10^4	5.64×10^3	1.03×10^4
Mn	6.49×10^3	*	2.30×10^3
Fe	1.03×10^5	*	6.76×10^4
Co	*	*	*
Ni	3.62×10^5	5.31×10^4	1.13×10^5
Rb	6.20×10^3	*	*
Zr	*	*	*
Mo	2.67×10^5	1.29×10^5	5.65×10^4
Ru	*	*	*
Rh	*	*	*
Pd	*	*	*

Re	*	*	*

** Concentrations were below LOD (1×10^3 µg/L).
*Concentrations were below LOD (2×10^3 µg/L).
[#] Concentrations had a 10% RSD.

3.3 Water Condenser

During Experiment 2, the volume of condensate collected in the water condenser graduated cylinder was tabulated in Table 5 and graphed in Figure 24. The collected solution was yellow. This coloration was likely due to the water condensate dissolving yellow solids coating the water condenser. Elements found on the condenser outlet, such as Cr, Mn, Fe, Ni, or Mo could be dissolved in the water condenser aliquot. Figure 24 suggested the rate of water generations was relatively linear; however, the percent conversion for Experiment 2 would suggest the rate of hydrochlorination decreased between the 4-h and 5-h timepoint. A consistent water generation could be rationalized by continued hydrochlorination while the drop in percent conversion could be explained by decomposition of water-soluble U species to uranium oxides.

Based on the free acid analysis of the water condenser aliquot, the acid normality was relatively high (Table 6). Presumably, the acidity was due to dissolved HCl.

Table 5. Volume of condensate collected in the graduated cylinder for Experiment 2.

Timepoint (h)	mL condensate
0.5	*
1	*
1.5	*
2	*
2.5	3.1
3	3.8
3.5	4.0
4	4.8
4.5	5.2
5	5.5

*Below quantitative volume.

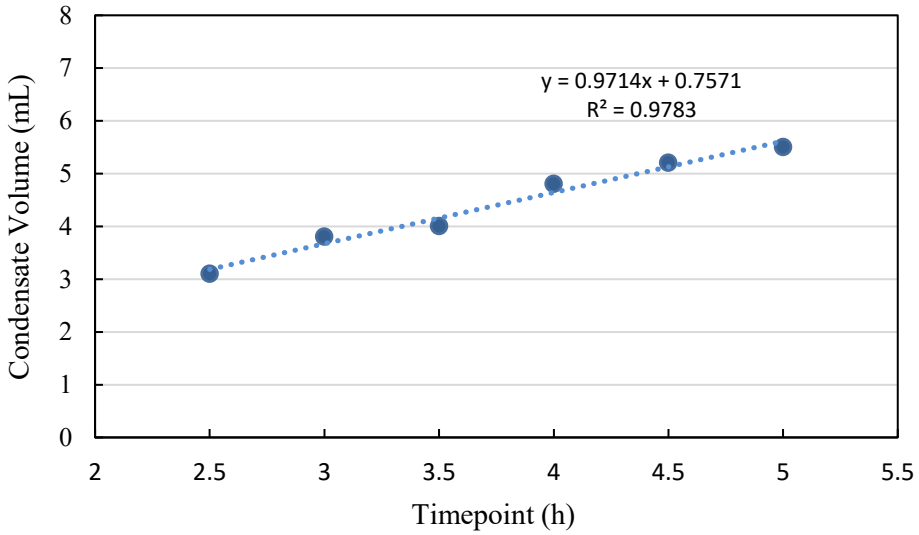

Figure 24. Condensate volume measured at regular intervals for Experiment 2.

Table 6. Free acid analysis of the water condenser aliquot for experiment 2.

Sample	Concentration (N)
Water Condenser Aliquot	10.4

3.4 Scrubber Bottles

The ICP-MS concentrations (Table A 8) of Total U for the scrubber bottles from Experiments 2-4 were relatively low (ranging from 1.08×10^2 to 6.49×10^3 µg/L). Experiment 5 scrubber bottles had total U concentrations below LOD. ICP-MS of the scrubber bottles for Experiment 4 at timepoints 4 and 6 h had Ni concentrations of 7.05×10^3 µg/L and 3.14×10^3 µg/L, respectively (Table A 9). The Experiment 5 scrubber bottle 1 had a W concentration of 1.09×10^3 µg/L. These results suggest relatively low amounts of U and corrosion species had made it through the off-gas system to the scrubber bottles.

An IC-Anions analysis revealed chloride was also present in the scrubber bottles (Table A 10). For Experiment 2 scrubber bottle 2, the compromised frit likely contributed to the chloride content being below the LOD. Several other anions, such as fluoride, formate, nitrite, nitrate, phosphate, sulfate, oxalate, and bromide concentrations were assessed as part of the IC-Anions analysis, but these anion concentrations were expectedly below LOD. NAA supported the presence of chloride in the scrubber bottles for Experiment 2 (Table A 11).

The high concentration of chloride in the scrubber bottles likely indicated neutralization of HCl gas by sodium hydroxide to form sodium chloride. Depending on the intermediates or side reactions occurring in the reaction mixture or off-gas system, chlorine gas may also be a component present in the scrubber bottle solutions. As hydrochlorination progressed, white solids were observed in the scrubber bottles. The solids were likely sodium chloride that precipitated or crystallized due to saturation of the scrubber bottle solutions. For Experiment 2, a 201 g/L chloride concentration was measured in scrubber bottle 1. Assuming the chloride concentration was sodium chloride, the concentration would be 331 g/L sodium chloride. The expected sodium chloride solubility in water is 357 g/L at 25 °C. Given laboratory temperatures may be lower than 25 °C, sodium chloride precipitation would be likely. Another potential product could be hypochlorite salts.

4.0 Conclusions

Though Phase 1 provided evidence of successful hydrochlorination, Phase 2 highlighted the nuances and challenges associated with scaling up the reaction. The target UCl_4 species generated by the hydrochlorination of UO_2 (Equation 1) also generates water, which consumes UCl_4. Compared to the single datapoint obtained at the end of the Phase 1 experiments, data collected at multiple timepoints during Phase 2 experiments indicated a presumed maximum percent conversion of 23% for this system that is likely influenced by water generation. Engineering improvements might be able to increase the percent conversion, but not likely to the degree needed for successful implementation of the technology. The water presents an issue for maintaining the integrity of for the Hastelloy C276 reaction vessel. Eventually, corrosion will compromise the integrity of the reaction vessel, and the corrosion products could potentially affect the hydrochlorination chemistry of UO_2. The presence of corrosion products, which were not produced in the Phase 1 alumina crucible, can and have created challenges when analyzing samples.

5.0 Recommendations, Path Forward or Future Work

Hydrochlorination of UO_2 using anhydrous HCl appears to be hindered by its own success through the generation of water. If continued focus on the target reaction is desired, managing water must be a priority to increase percent conversion and reduce corrosion of the Hastelloy C276 vessel. Regardless, aside from a perfect exclusion of water, the effects of moisture on the current system will eventually compound. Given the current challenges related to the chemistry of the reaction, an engineering solution would not likely not solve this system's current issues. An alternative reaction that does not generate water would be recommended. Carbon tetrachloride and phosgene are two chemicals which have been shown to be effective at converting UO_2 to UCl_4 without the generation of water.

6.0 References

1 Baer, D. K. System and Methods for Fast Molten Salt Reactor Fuel-Salt Preparation. United States of America patent US 11062813 B2 (2021).

2 Volkovich, V. A., Bhatt, A. I., May, I., Griffiths, T. R. & Thied, R. C. A Spectroscopic Study of Uranium Species Formed in Chloride Melts. *Journal of Nuclear Science and Technology* **39**, 595-598 (2002). https://doi.org:10.1080/00223131.2002.10875538

3 Volkovich, V. A. *et al.* Effect of Melt Composition on the Reaction of Uranium Dioxide with Hydrogen Chloride in Molten Alkali Chlorides. **62**, 671-676 (2007). https://doi.org:doi:10.1515/zna-2007-10-1116

4 Nguyen, V. T., Foley, B. J. & Pierce, R. A. "Hydrochlorination of Uranium Dioxide in a Molten Salt Mixture - Phase 1: Tube Furnace Cross Flow Experiments" SRNL-TR-2024-00718, Rev. 0, October 2024.

5 Kittel, J. H., Horak, J. A., Beck, W. N. & Fousek, R. J. Irradiation Behavior of Uranium-Fissium Alloys. Report No. ANL-6795, (ANL, 1971).

6 Group, F. R. W. Nuclear Metal Fuel: Characteristics, Design, Manufacturing, Testing, and Operating History. 1-33 (2018).

7 Salyulev, A. B., Kudyakov, V. Y. & Moskalenko, N. I. Volatilities of the Components of the Saturated Vapors of UCl4 Solutions in a Molten Equimolar NaCl–KCl Mixture. *Russian Metallurgy (Metally)* **2021**, 992-997 (2021). https://doi.org:10.1134/S0036029521080176

8 Kraus, K. A. & Nelson, F. Hydrolytic Behavior of Metal Ions. I. The Acid Constants of Uranium(IV) and Plutonium(IV)1. *Journal of the American Chemical Society* **72**, 3901-3906 (1950). https://doi.org:10.1021/ja01165a020

9 Hearne, J. A. & White, A. G. 400. The heat of solution of uranium tetrachloride and the hydrolysis of the uranium(IV) ion. *Journal of the Chemical Society (Resumed)*, 2081-2085 (1957). https://doi.org:10.1039/JR9570002081

10 Naumann, D., Tschirne, G. & Burk, W. Über das Hydrolyseverhalten von Urantetrachlorid in Alkalichloridschmelzen. *Zeitschrift für anorganische und allgemeine Chemie* **332**, 63-68 (1964). https://doi.org:https://doi.org/10.1002/zaac.19643320108

11 Branch, S. D., Felmy, H. M., Schafer Medina, A., Bryan, S. A. & Lines, A. M. Exploring the Complex Chemistry of Uranium within Molten Chloride Salts. *Industrial & Engineering Chemistry Research* **62**, 14901-14909 (2023). https://doi.org:10.1021/acs.iecr.3c02005

12 Haas, P. A., Lee, D. D. & Mailen, J. C. Reaction of uranium oxides with chlorine and carbon or carbon monoxide to prepare uranium chlorides. (United States, 1991).

13 Kanellakopulos, B. & Parthey, H. The oxidation of uranium tetrachloride. *Journal of Inorganic and Nuclear Chemistry* **28**, 2541-2549 (1966). https://doi.org:https://doi.org/10.1016/0022-1902(66)80378-0

14 Sinkov, S. I., Hall, G. B. & Lumetta, G. J. Molar absorptivities of U(VI), U(IV), and Pu(III) in nitric acid solutions of various concentrations relevant to developing nuclear fuel recycling flowsheets. *Journal of Radioanalytical and Nuclear Chemistry* **324**, 773-789 (2020). https://doi.org:10.1007/s10967-020-07106-8

15 Hege, N., Jackson, J. A. & Shafer, J. C. Review—Fundamental Uranium Electrochemistry and Spectroscopy in Molten Salt Systems. *J. Electrochem. Soc.* **170**, 1-19 (2023). https://doi.org:10.1149/1945-7111/acafa9

Appendix A. Additional Data

Table A 1. Masses and moles of UO_2, NaCl, CsCl, and fissium compounds.

Experiment 1			
Compound	Mass (g)	Moles	Mol%
NaCl	71.579	1.22	24.4
CsCl	383.030	2.27	45.5
UO_2	404.9955	1.50	30.1
Total	859.605	4.99	100.0
Experiment 2			
Compound	Mass (g)	Moles	Mol%
NaCl	71.656	1.23	24.6
CsCl	383.974	2.27	45.4
UO_2	404.9718	1.50	30.0
Total	859.602	5.00	100.0
Experiment 3			
Compound	Mass (g)	Moles	Mol%
NaCl	108.969	1.86	33.6
CsCl	583.490	3.46	62.6
UO_2	55.9994	0.21	3.8
Total	748.4584	5.54	100.0
Experiment 4			
Compound	Mass (g)	Mass%	Moles
NaCl	71.616	8.33	1.225
CsCl	382.981	44.56	2.275
UO_2	404.9422	47.11	0.667
MoO_3	11.563	1.35	0.080
PdO	0.780	0.09	0.006
$ReO_2 \cdot 2H_2O$	0.681	0.08	0.003
Rh_2O_3 Hydrate	0.308	0.04	0.002
$Ru(NO_3)(NO)$	1.297	0.15	0.004
ZrO_2	6.13	0.71	0.050
Total	874.486	100	2.477
Experiment 5			
Compound	Mass (g)	Moles	
NaCl (in frit)	17.885	0.31	
CsCl (in frit)	95.707	0.57	
UO_2 (in frit)	101.2769	0.38	
NaCl (in vessel liner)	76.712	1.31	
CsCl (in vessel liner)	410.421	2.44	
Total	702.0019	5.01	

Table A 2. Masses of empty centrifuge tube, water, and molten salt samples.

Experiment 1					
Timepoint (h)	Empty tube (g)	Tube + water (g)	Tube + water + sample (g)	Water (g)	Sample weight (g)
0.5	13.2623	33.2730	34.1763	20.0107	0.9033
1	13.3018	33.2977	*	19.9959	*
1.5	13.3140	33.3130	34.5332	19.9990	1.2202
2	13.2899	33.2809	33.6710	19.9910	0.3901
2.5	13.2397	33.2400	34.7358	20.0003	1.4958
3	13.3087	33.3129	34.5599	20.0042	1.2470
3.5	13.3105	33.3431	34.6735	20.0326	1.3304
4	13.2746	33.2871	34.2953	20.0125	1.0082
4.5	13.2334	33.2413	34.3582	20.0079	1.1169
5	13.3278	33.3364	34.3096	20.0086	0.9732
5.5	13.0754	33.0859	33.6441	20.0105	0.5582
6	13.2697	33.2751	38.5398	20.0054	5.2647
Experiment 2					
Timepoint (h)	Empty tube (g)	Tube + water (g)	Tube + water + sample (g)	Water (g)	Sample weight (g)
0.5	13.1304	32.1002	34.1386	18.9698	2.0384
1	13.2848	32.5400	33.5160	19.2552	0.9760
1.5	13.2259	32.4255	33.0032	19.1996	0.5777
2	13.0837	32.3161	33.4726	19.2324	1.1565
2.5	13.1274	32.3237	33.8232	19.1963	1.4995
3	13.1120	32.4683	33.6972	19.3563	1.2289
3.5	13.2940	32.6248	33.5942	19.3308	0.9694
4	13.3240	32.4031	33.0230	19.0791	0.6199
4.5	13.4843	32.7340	33.4731	19.2497	0.7391
5	13.3466	32.5934	33.6952	19.2468	1.1018
Experiment 3					
Timepoint (h)	Empty tube (g)	Tube + water (g)	Tube + water + sample (g)	Water (g)	Sample weight (g)
0.5	13.1351	32.9992	35.1467	19.8641	2.1475
1	13.5102	33.1573	35.8367	19.6471	2.6794
1.5	13.5057	33.5085	35.2405	20.0028	1.732
2	13.3773	33.351	35.256	19.9737	1.905
2.5	13.5256	33.6247	35.3995	20.0991	1.7748
3	13.4135	33.4017	35.3576	19.9882	1.9559
3.5	13.5029	33.5076	35.5181	20.0047	2.0105

4	13.4593	33.4202	35.0924	19.9609	1.6722
4.5	13.4931	33.4018	35.1802	19.9087	1.7784
5	13.2707	33.1824	34.6802	19.9117	1.4978
5.5	13.5412	33.4204	35.044	19.8792	1.6236
6 (Day 1)	13.5433	33.4759	34.9267	19.9326	1.4508
6 (Day 2)	13.5419	33.5911	35.3285	20.0492	1.7374
7	13.4348	33.5453	34.9316	20.1105	1.3863
8	13.4012	33.5368	34.8663	20.1356	1.3295
9	13.4745	33.5764	34.9274	20.1019	1.351
10	13.4653	33.584	35.2296	20.1187	1.6456
11	13.4135	33.5703	35.2406	20.1568	1.6703
12	13.2267	33.2671	33.7103	20.0404	0.4432
Experiment 4					
Timepoint (h)	Empty tube (g)	Tube + water (g)	Tube + water + sample (g)	Water (g)	Sample weight (g)
1	13.675	33.672	35.1803	19.997	1.508
2	13.286	33.288	35.1966	20.002	1.909
3	13.317	33.336	34.8798	20.019	1.544
4	13.503	33.475	34.8780	19.972	1.403
5	13.681	33.651	34.8138	19.970	1.163
6	13.451	33.428	34.8313	19.977	1.403
Experiment 5					
Timepoint (h)	Empty tube (g)	Tube + water (g)	Tube + water + sample (g)	Water mass (g)	Sample weight (g)
0.75	13.5696	33.6096	35.7071	20.0400	2.0975
1.5	13.4477	33.3669	35.4026	19.9192	2.0357
2.25	13.4044	33.3065	34.7113	19.9021	1.4048
3	13.5536	33.4625	35.3617	19.9089	1.8992
3.75	13.5359	33.448	34.8379	19.9121	1.3899
4.5	13.5425	33.5624	35.5461	20.0199	1.9837
5.25	13.5042	33.5003	34.9329	19.9961	1.4326
6	13.4594	33.4723	34.8353	20.0129	1.3630

*Data not collected.

Table A 3. Uranium isotope concentrations as determined by ICP-MS.**

Experiment 1			
Timepoint (h)	U-235 (µg/L)	U-238 (µg/L)	Total U (µg/L)
6	*	1.20×10^{4}	1.20×10^{4}
Experiment 2			
Timepoint (h)	U-235 (µg/L)	U-238 (µg/L)	Total U (µg/L)
1	1.32×10^{3}	6.80×10^{5}	6.82×10^{5}
2	2.88×10^{3}	1.50×10^{6}	1.50×10^{6}
3	5.62×10^{3}	2.90×10^{6}	2.91×10^{6}
4	5.11×10^{3}	2.65×10^{6}	2.66×10^{6}
5	9.55×10^{3}	4.91×10^{6}	4.92×10^{6}
Experiment 3			
Timepoint (h)	U-235 (µg/L)	U-238 (µg/L)	Total U (µg/L)
1	1.15×10^{2}	6.62×10^{4}	6.63×10^{4}
2	3.49×10^{2}	1.84×10^{5}	1.84×10^{5}
3	6.39×10^{2}	3.36×10^{5}	3.36×10^{5}
4	8.03×10^{2}	4.06×10^{5}	4.07×10^{5}
5	9.21×10^{2}	4.83×10^{5}	4.84×10^{5}
6	9.81×10^{2}	5.15×10^{5}	5.13×10^{5}
7	1.25×10^{3}	6.34×10^{5}	6.35×10^{5}
8	1.32×10^{3}	6.81×10^{5}	6.82×10^{5}
9	1.54×10^{3}	8.58×10^{5}	8.60×10^{5}
10	1.98×10^{3}	1.09×10^{6}	1.09×10^{6}
11	1.72×10^{3}	9.39×10^{5}	9.41×10^{5}
12	3.99×10^{2}	2.23×10^{5}	2.24×10^{5}
Experiment 4			
Timepoint (h)	U-235 (µg/L)	U-238 (µg/L)	Total U (µg/L)
1	*	2.21×10^{3}	2.21×10^{3}
2	*	*	-
3	*	1.77×10^{5}	1.77×10^{5}
4	1.54×10^{4}	7.88×10^{5}	8.03×10^{5}
5	*	4.87×10^{5}	4.87×10^{5}
6	1.41×10^{3}	7.36×10^{5}	7.37×10^{5}
Experiment 5			
Timepoint (h)	U-235 (µg/L)	U-238 (µg/L)	Total U (µg/L)
0.75	3.36×10^{2}	1.81×10^{5}	1.81×10^{5}
1.5	6.29×10^{2}	3.22×10^{5}	3.23×10^{5}
2.25	7.20×10^{2}	3.69×10^{5}	3.70×10^{5}
3	1.07×10^{3}	5.35×10^{5}	5.36×10^{5}

3.75	9.71×10^{2}	4.53×10^{5}	4.54×10^{5}
4.5	1.18×10^{3}	6.10×10^{5}	6.12×10^{5}
5.25	1.06×10^{3}	5.42×10^{5}	5.43×10^{5}
6	1.04×10^{3}	5.30×10^{5}	5.31×10^{5}

*Concentrations were below LOD. For Experiment 1 and Experiment 4, LOD values were below 100 µg/L and 1000 µg/L, respectively. All concentrations for U-235 and U-238 had 2 sigma % UNC were 20%.
**Note: the total U concentrations do not account for variations in the mass of the dip sample or the volume of water used for dissolution and, as a result, should not be used for comparisons.

Equation A1

$$Total\ U\left(\frac{\mu g}{L}\right) = \text{Conc U 235}\left(\frac{\mu g}{L}\right) + \text{Conc U 238}\left(\frac{\mu g}{L}\right)$$

Table A 4. Elemental concentrations (µg/L) of the Experiment 3 dip sample at timepoint 12 h.

Element	Concentration (µg/L)
Ni	1.75×10^{6}
Cr	3.32×10^{5}
Fe	1.96×10^{5}
Mn	1.77×10^{4}
Co	6.20×10^{3}
Mo	2.81×10^{3}

Table A 5. Elemental concentrations (µg/L) of Experiment 4 dip samples were measured with a 10% RSD.

Element	1 h	2 h	3 h	4 h	5 h	6 h
Cr	2.51×10^{3}	*	1.71×10^{5}	2.89×10^{5}	2.53×10^{5}	3.86×10^{5}
Mn	4.28×10^{3}	7.65×10^{3}	2.30×10^{4}	2.44×10^{4}	2.28×10^{4}	2.95×10^{4}
Fe	*	6.77×10^{4}	4.25×10^{5}	6.90×10^{5}	5.84×10^{5}	8.21×10^{5}
Co	*	2.42×10^{3}	3.72×10^{3}	4.10×10^{3}	4.14×10^{3}	5.52×10^{3}
Ni	2.81×10^{5}	4.27×10^{5}	8.11×10^{5}	1.02×10^{6}	1.06×10^{6}	1.55×10^{6}
Rb	5.19×10^{4}	6.71×10^{4}	5.15×10^{4}	4.83×10^{4}	3.73×10^{4}	4.69×10^{4}
Zr	*	*	*	*	*	*
Mo	5.14×10^{5}	9.52×10^{5}	9.61×10^{4}	1.79×10^{5}	9.53×10^{4}	1.22×10^{5}
Ru	4.15×10^{3}	*	6.28×10^{3}	5.60×10^{3}	*	*
Rh	*	*	*	*	*	*
Pd	*	*	*	*	*	*
Re	6.35×10^{4}	7.34×10^{4}	6.88×10^{3}	*	*	*

*Concentrations were below LOD (2×10^{3} µg/L).

Table A 6. Elemental concentrations (µg/L) of Experiment 5 dip samples with a 10% RSD.

Element	0.75 h	1.5 h	2.25 h	3 h	3.75 h	4.5 h	5.25 h	6 h
Cr	2.72×10^{5}	4.72×10^{5}	4.42×10^{5}	6.22×10^{5}	5.36×10^{5}	7.36×10^{5}	6.60×10^{5}	6.92×10^{5}
Mn	5.63×10^{3}	7.27×10^{3}	7.13×10^{3}	1.12×10^{4}	9.97×10^{3}	1.44×10^{4}	1.32×10^{4}	1.44×10^{4}
Fe	2.55×10^{5}	3.65×10^{5}	3.25×10^{5}	4.46×10^{5}	3.67×10^{5}	5.01×10^{5}	4.27×10^{5}	4.56×10^{5}
Co	1.01×10^{4}	1.54×10^{4}	1.39×10^{4}	1.88×10^{4}	1.56×10^{4}	2.10×10^{4}	1.77×10^{4}	1.85×10^{4}
Ni	9.38×10^{5}	1.26×10^{6}	1.12×10^{6}	1.75×10^{6}	1.54×10^{6}	2.12×10^{6}	1.90×10^{6}	2.03×10^{6}
Rb	9.14×10^{4}	8.82×10^{4}	6.75×10^{4}	8.27×10^{4}	6.27×10^{4}	7.98×10^{4}	6.44×10^{4}	6.22×10^{4}
Mo	7.22×10^{4}	4.54×10^{4}	4.01×10^{4}	5.56×10^{4}	4.68×10^{4}	5.89×10^{4}	5.61×10^{4}	6.82×10^{4}
W	4.34×10^{4}	3.05×10^{3}	1.28×10^{3}	1.76×10^{3}	1.57×10^{3}	*	*	1.95×10^{3}

*Concentrations were below LOD (1×10^{3} µg/L).

Table A 7. Normalized Concentration (ppm/g dip sample) of Experiment 5 dip samples using concentrations from Table A 6.

Normalized Concentration [(ug/L) / g dip sample]									
Time (min)	Cr	Mn	Fe	Co	Ni	Rb	Mo	W	U
45	1.30×10^{5}	2.68×10^{3}	1.21×10^{5}	4.83×10^{3}	4.47×10^{5}	4.36×10^{4}	3.44×10^{4}	2.07×10^{3}	1.35×10^{5}
90	2.32×10^{5}	3.57×10^{3}	1.79×10^{5}	7.55×10^{3}	6.18×10^{5}	4.33×10^{4}	2.23×10^{4}	1.50×10^{3}	2.39×10^{5}
135	3.14×10^{5}	5.07×10^{3}	2.32×10^{5}	9.91×10^{3}	7.99×10^{5}	4.81×10^{4}	2.86×10^{4}	9.10×10^{2}	3.24×10^{5}
180	3.27×10^{5}	5.90×10^{3}	2.35×10^{5}	9.91×10^{3}	9.21×10^{5}	4.35×10^{4}	2.93×10^{4}	9.27×10^{2}	3.37×10^{5}
225	3.85×10^{5}	7.17×10^{3}	2.64×10^{5}	1.12×10^{4}	1.11×10^{6}	4.51×10^{4}	3.36×10^{4}	1.13×10^{3}	3.97×10^{5}
270	3.71×10^{5}	7.26×10^{3}	2.52×10^{5}	1.06×10^{4}	1.07×10^{6}	4.02×10^{4}	2.97×10^{4}	-	3.82×10^{5}
315	4.61×10^{5}	9.20×10^{3}	2.98×10^{5}	1.24×10^{4}	1.33×10^{6}	4.50×10^{4}	3.91×10^{4}	-	4.73×10^{5}
360	5.08×10^{5}	1.06×10^{4}	3.35×10^{5}	1.36×10^{4}	1.49×10^{6}	4.57×10^{4}	5.01×10^{4}	1.43×10^{3}	5.21×10^{5}

Table A 8. Uranium isotopics as determined by ICP-MS of scrubber bottles.[#]

Experiment 2- Scrubber Bottle 1			
Timepoint (h)	U-235 (µg/L)	U-238 (µg/L)	Total U (µg/L)
2	4.30×10^{2}	1.31×10^{3}	1.74×10^{3}
4	6.49×10^{2}	1.81×10^{3}	2.46×10^{3}
5	6.26×10^{2}	1.87×10^{3}	2.50×10^{3}
Experiment 3- Scrubber Bottle 1			
Timepoint (h)	U-235 (µg/L)	U-238 (µg/L)	Total U (µg/L)
2	*	**	-
4	1.27×10^{3}	**	1.27×10^{3}
6	1.08×10^{2}	**	1.08×10^{2}
Experiment 4- Scrubber Bottle 1			
Timepoint (h)	U-235 (µg/L)	U-238 (µg/L)	Total U (µg/L)
2	**	**	-
4	**	**	-
6	1.05×10^{3}	3.14×10^{3}	4.19×10^{3}
Experiment 5- Scrubber Bottle 1			
Timepoint (h)	U-235 (µg/L)	U-238 (µg/L)	Total U (µg/L)
3	*	$<2\times10^{2}$	-
Experiment 5- Scrubber Bottle 2			
Timepoint (h)	U-235 (µg/L)	U-238 (µg/L)	Total U (µg/L)
3	*	$<2\times10^{2}$	-
6	*	$<2\times10^{2}$	-

*Concentrations were below LOD (1×10^{2} µg/L).
**Concentrations were below LOD (1×10^{3} µg/L).
[#]Concentrations had a 10% RSD.

Table A 9. Concentration of elements (µg/L) and (%RSD) measured in scrubber bottles, as determined by ICP-MS.

Element	Exp 4-Scrubber Bottle 1			Exp 5- Scrubber Bottle 1	Exp 5- Scrubber Bottle 2	
	2 h	4 h	6 h	3 h	3 h	6 h
Cr	$< 2.00\times10^3$	$< 2.00\times10^3$	$< 1.00\times10^3$	$< 1.00\times10^3$	$< 1.00\times10^3$	$< 1.00\times10^3$
Mn	$< 2.00\times10^3$	$< 2.00\times10^3$	$< 1.00\times10^3$	$< 1.00\times10^3$	$< 1.00\times10^3$	$< 1.00\times10^3$
Fe	$< 2.00\times10^3$	$< 2.00\times10^3$	$< 1.05\times10^3$	$< 1.00\times10^4$	$< 1.00\times10^4$	$< 1.00\times10^4$
Co	$< 2.00\times10^3$	$< 2.00\times10^3$	$< 1.00\times10^3$	$< 1.00\times10^1$	$< 1.00\times10^2$	$< 1.00\times10^2$
Ni	$< 2.00\times10^3$	7.05×10^3	2.46×10^3	$< 1.00\times10^3$	$< 1.00\times10^3$	$< 1.00\times10^3$
Rb	$< 2.00\times10^3$	$< 2.00\times10^3$	$< 2.00\times10^3$	$< 1.00\times10^3$	$< 1.00\times10^3$	$< 1.00\times10^3$
Zr	$< 2.00\times10^3$	$< 2.00\times10^3$	$< 2.00\times10^3$	$< 1.00\times10^3$	$< 1.00\times10^3$	$< 1.00\times10^3$
Nb	$< 2.00\times10^3$	$< 2.00\times10^3$	$< 2.00\times10^3$	$< 1.00\times10^3$	$< 1.00\times10^3$	$< 1.00\times10^3$
Mo	$< 2.00\times10^3$	$< 2.00\times10^3$	$< 2.00\times10^3$	$< 1.00\times10^3$	$< 1.00\times10^3$	$< 1.00\times10^3$
Ru	$< 2.00\times10^3$	$< 2.00\times10^3$	$< 2.46\times10^3$	$< 1.00\times10^3$	$< 1.00\times10^3$	$< 1.00\times10^3$
Rh	$< 2.00\times10^3$	$< 2.00\times10^3$	$< 2.00\times10^3$	$< 1.00\times10^3$	$< 1.00\times10^3$	$< 1.00\times10^3$
Pd	$< 2.00\times10^3$	$< 2.00\times10^3$	$< 2.00\times10^3$	$< 1.00\times10^3$	$< 1.00\times10^3$	$< 1.00\times10^3$
Re	$< 2.00\times10^3$	$< 2.00\times10^3$	$< 2.00\times10^3$	$< 1.00\times10^3$	$< 1.00\times10^3$	$< 1.00\times10^3$
W				1.09×10^3 (10)	$< 1.00\times10^3$	$< 1.00\times10^3$

Table A 10. Chloride concentration (mg/L), as determined by IC-Anions, for the scrubber solutions and water condenser aliquot.[#]

Experiment 2			
Timepoint (h)	Scrubber Bottle 1	Scrubber Bottle 2	Water Condenser Aliquot
2	65600		
4	188000		
5	201000		582000
Experiment 3			
Timepoint (h)	Scrubber Bottle 1	Scrubber Bottle 2	Water Condenser Aliquot
2	45800	*	
4	92100	*	
6	182000	*	
Experiment 4			
Timepoint (h)	Scrubber Bottle 1	Scrubber Bottle 2	Water Condenser Aliquot
2	***	26800	
4	125000	***	
6	199000	***	441000
Experiment 5			
Timepoint (h)	Scrubber Bottle 1	Scrubber Bottle 2	Water Condenser Aliquot
3	140000	**	
6		89700	318000

*Concentrations were below LOD (10 µg/L).
**Concentrations were below LOD (1×10^2 µg/L).
***Concentrations were below LOD (1×10^3 µg/L).
[#]Concentrations had a 10% RSD.

Table A 11. Chloride concentration (µg/g) and (%RSD) of the two scrubber bottle solutions, as determined by neutron activation analysis (NAA) for Experiment 2.

Timepoint (h)	Scrubber Bottle 1	Scrubber Bottle 2
2	4.70×10^4 (5)	$< 5.39\times10^2$
4	1.20×10^5 (5)	$< 5.00\times10^2$
5	1.28×10^5 (5)	$< 4.99\times10^2$

Distribution:

Metatomic® Inc.:
Ken Baer (k.baer@metatomicenergy.com)
Tom Epting (t.epting@metatomicenergy.com)
Steve Hung (s.hung@metatomicenergy.com)
Tor Osmundsen (t.osmundsen@metatomicenergy.com)
Mike Stake (m.stake@metatomicenergy.com)

SRNL:
Vinh.nguyen@srnl.doe.gov
Nicole.hege@srnl.doe.gov
Bryan.foley@srnl.doe.gov
Robert.pierce@srnl.doe.gov
Thomas.Shehee@srnl.doe.gov
William.bates@srnl.doe.gov
utopia.boynton@srnl.doe.gov
Tyler.chavous@srnl.doe.gov
Brandi.clark@srnl.doe.gov
marion.cofer@srnl.doe.gov
Vanessa.cofer@srnl.doe.gov
alex.cozzi@srnl.doe.gov
c.diprete@srnl.doe.gov
David.diprete@srnl.doe.gov
connie.herman@srnl.doe.gov
sarah.hodges@srnl.doe.gov
Charles.James@SRNL.DOE.GOV
brady.lee@srnl.doe.gov
Heather.Capogreco@srnl.doe.gov
Joseph.Manna@srnl.doe.gov
Gregg.Morgan@srnl.doe.gov
frank.pennebaker@srnl.doe.gov
Amy.Ramsey@srnl.doe.gov
William.Ramsey@srnl.doe.gov
luther.reid@srnl.doe.gov
eric.skidmore@srnl.doe.gov
michael.stone@srnl.doe.gov
boyd.Wiedenman@srnl.doe.gov
Mary.whitehead@srnl.doe.gov
Morgana.whiteside@srnl.doe.gov
Jennifer.Wohlwend@srnl.doe.gov
Records Administration (EDWS)